

# The "Sources" of Plasma Physics

Francis F. Chen, *Fellow, IEEE*

(Invited Review Paper)

**Abstract**—This paper is the text of the Plasma Science and Applications Committee Prize address given in Santa Fe, NM, on June 7, 1994. The principal thesis is that major advances in the development of the science of plasmas have frequently been triggered by the invention of a new plasma source. Examples are given from the work of many colleagues in basic plasma research. A retrospective of the author's experiments on basic plasma physics, magnetic fusion, and inertial fusion is given, many of these sharing the common theme of transverse electric fields. The author's present and future work concern new plasma sources that are needed for the application of plasma technology to materials processing.

## I. INTRODUCTION

THE science of plasmas has grown enormously over the past forty years, and the key to the expansion of our knowledge about plasma behavior has been the discovery of new, better ways to create plasmas. The development of basic plasma physics can actually be traced through the invention of new sources, which each time triggered new insights into the behavior of plasmas. In Section II, I shall give a few selected examples of such break-through plasma sources and the classic experiments that resulted from them. This section will include not only my own work but also that of others. I take this opportunity to honor my colleagues who, over the years, have joined me in the mission to establish and solidify the foundations of modern plasma physics through inspired experimentation. In Section III, I shall discuss a number of experiments, mostly my own, including unpublished ones, which are tied together through a common theme, that of transverse electric fields. Finally, Section IV will project what the technological plasma sources of the future will do for our science.

## II. BREAK-THROUGH PLASMA SOURCES

### A. Duoplasmatron Source

Fig. 1 shows the Duoplasmatron source of Boeschoten and Schwirzke [1]. The plasma is created in a small filament discharge at 40 mTorr of  $H$  and injected through a 1–3 mm diam hole through a magnetic mirror into the main chamber,

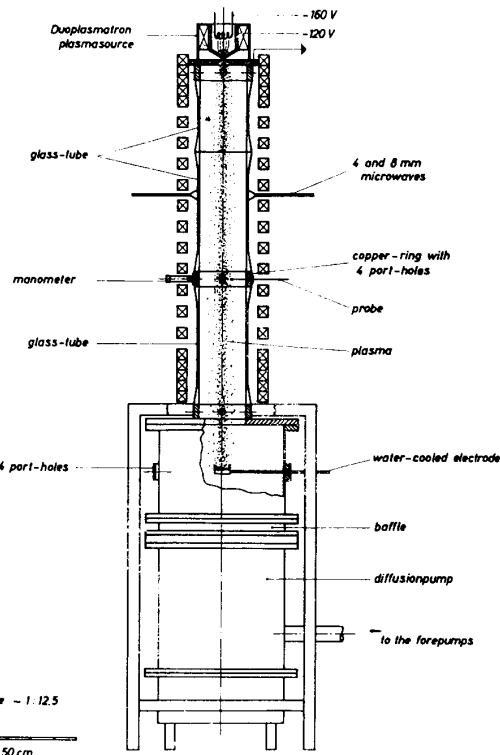


Fig. 1. The duoplasmatron source [1].

Fig. 1. The duoplasmatron source [1].

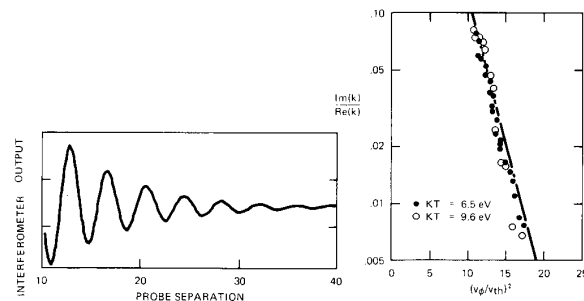


Fig. 2. The Malmberg-Wharton experiment on Landau damping [2].

which is 120 cm long, with a magnetic field of up to 4 kG and pressures as low as  $10^{-5}$  Torr. The small-diameter plasma was quiescent enough for basic experiments on electrons. No one

Manuscript received September 28, 1994; revised November 30, 1994.  
The author is with the Electrical Engineering Department, University of California at Los Angeles, Los Angeles, CA 90024-1594 USA.  
IEEE Log Number 9408679.

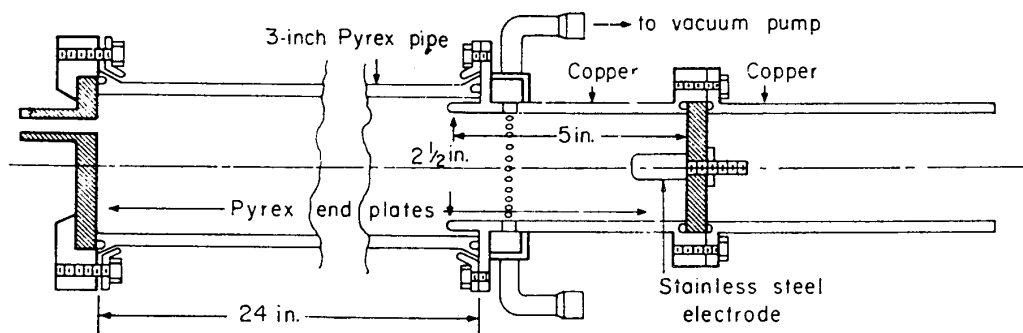
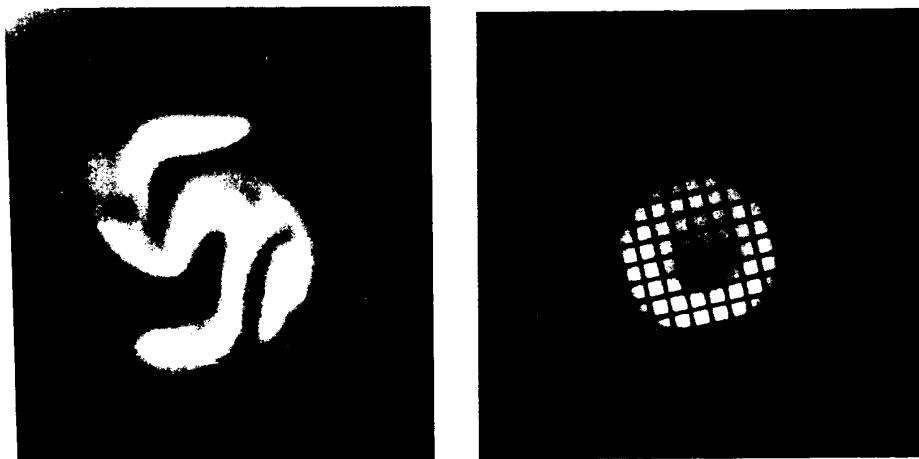
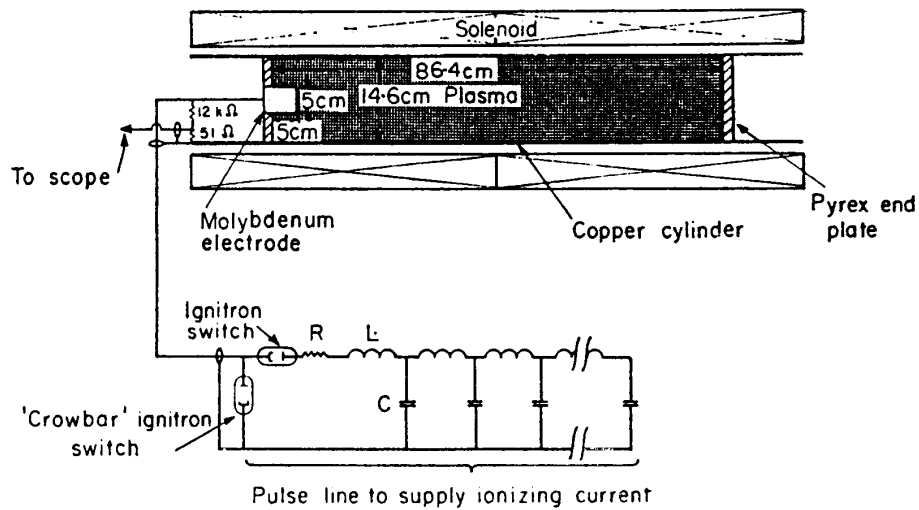


Fig. 3. The "hot house" discharge [3]. Axial views of unstable and stable plasmas are shown, as well as the grid modification used for stabilization.

knows why the plasma was more stable than in other sources; perhaps it was ion FLR stabilization or favorable curvature in the source region. The most famous result arising from this source is, of course, Malmberg and Wharton's demonstration of electron Landau damping [2]. This was reported at the IAEA meeting in London, UK, in the early 1960's, and the familiar result is shown in Fig. 2. The amplitude was shown to decay

exponentially as predicted. Up to this time there was doubt as to whether Landau damping was a real effect, since it was not clear that electrons could follow a Maxwellian distribution as closely as the theory required; that they do so is still a puzzle, called Langmuir's paradox. This experiment was an important demonstration, and it succeeded because the duoplasmatron source could provide a suitable plasma.

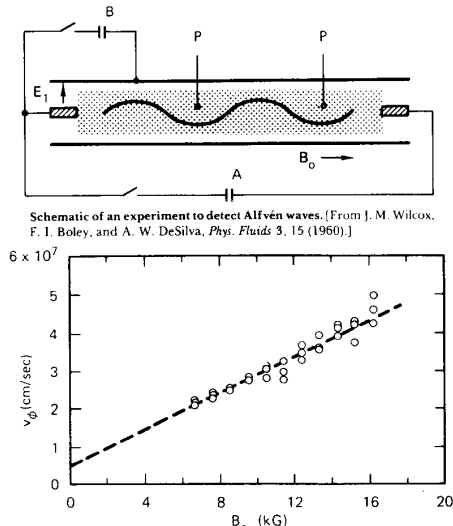


Fig. 4. The Alfvén wave experiment at Berkeley [4].

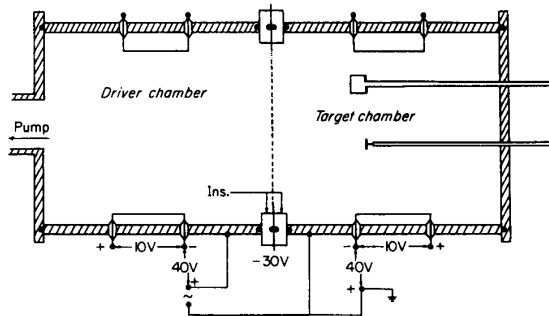


Fig. 5. The double-plasma device [5].

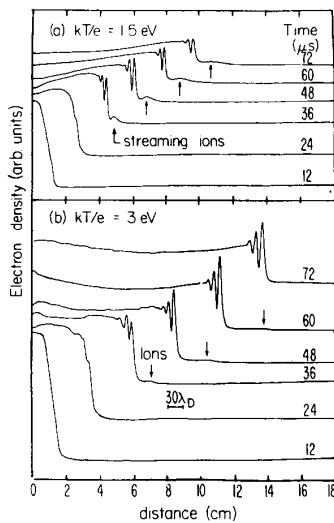


Fig. 6. Observation of ion acoustic shock waves [6].

**B. The "Hot-House" Discharge**

The first verification of Alfvén waves was made possible by a very special plasma which could produce  $10^{15} \text{ cm}^{-3}$

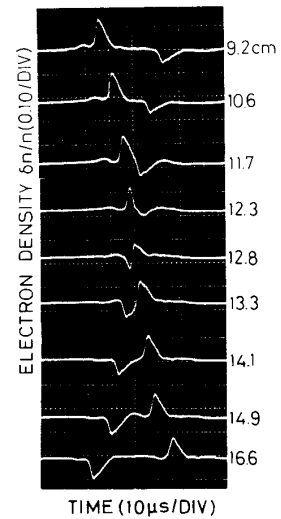
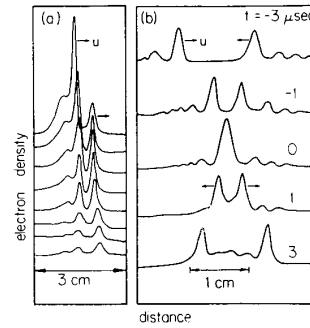


Fig. 7. Collision of solitons [7].

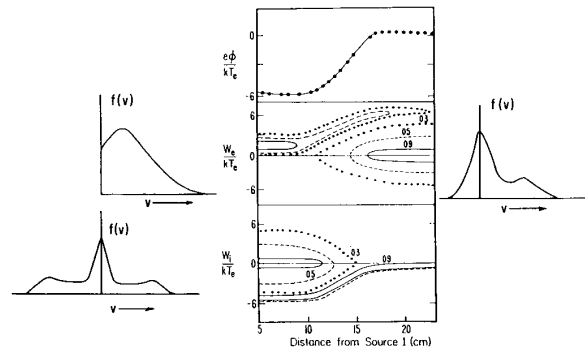


Fig. 8. Distribution functions in a double layer [8].

densities in hydrogen at 10 kG. This was the "hot-house" discharge, or slow pinch, developed by Bill Baker at U.C. Berkeley, CA, using a slow capacitor bank to drive a current between two endplates without actually pinching the plasma. Torsional Alfvén modes were excited with a ringing capacitor bank applied between a central electrode and the wall. The high density was necessary to slow down the wave to fit between the endplates, and the high magnetic field and light ion mass were necessary to minimize the damping. Fig. 3

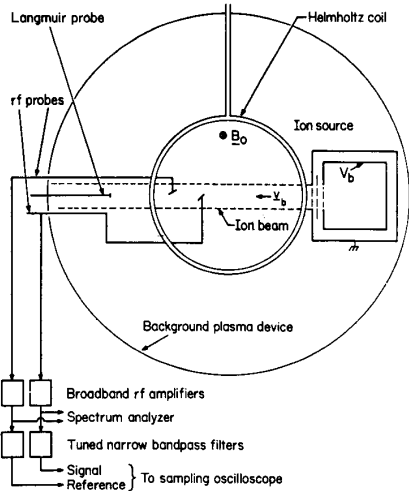


Fig. 9. Electron cyclotron drift wave experiment using a double plasma [9].

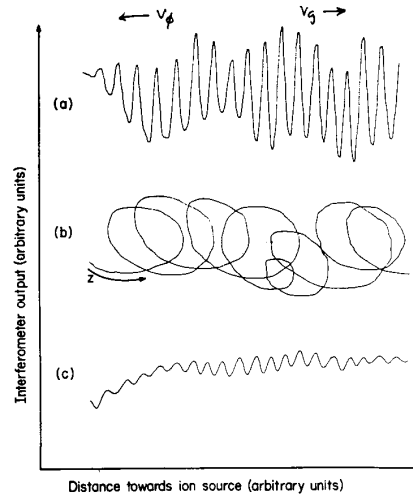


Fig. 11. Demonstration of backward waves [9].

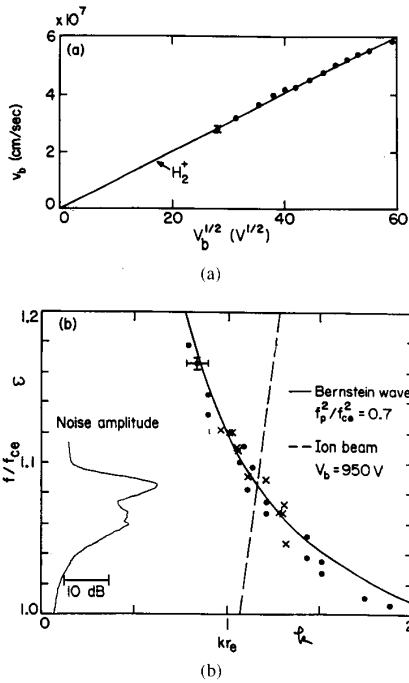


Fig. 10. Measured dispersion relation of electron Bernstein wave [9]. Solid line: Bernstein wave; dash line: ion beam velocity.

from the paper of Wilcox *et al.* [3] shows that producing a good plasma was not simple; instabilities would occur without certain modifications. Fig. 4 shows the experiment of Wilcox, Boley, and deSilva [4] *et al.*, verifying the constancy of the Alfvén velocity. A similar experiment was also done in England by Jephcott.

C. The Double-Plasma Device

Experimental nonlinear plasma physics had its roots in the invention of the double-plasma machine by Taylor, MacKen-

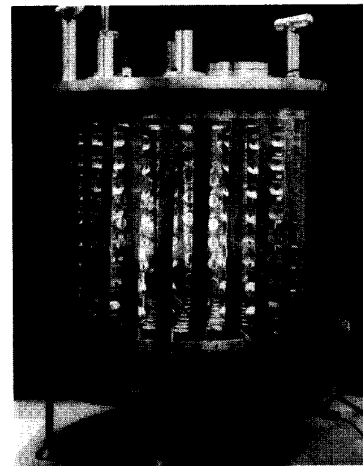


Fig. 12. A multipole confinement chamber (MacKenzie bucket, courtesy of R. L. Stenzel).

zie, and Ikezi [5]. By separating two filament discharges with a grid and applying a bias voltage between the two chambers, one can cause plasma to stream from one discharge into the other at velocities exceeding the sound velocity. Ion acoustic shock waves could be studied for the first time. The device is shown in Fig. 5, and the classic shock wave structure predicted by Sagdeev, as measured by Taylor, Baker, and Ikezi [6], is shown in Fig. 6. Double and triple plasmas have since been used to see such phenomena as solitons and double layers, the latter of importance in ionospheric physics. Fig. 7 shows the collision (or lack of one) of two Korteweg-deVries solitons seen by Ikezi, Taylor, and Baker [7], and Fig. 8 shows the distribution functions measured by Quon and Wong [8] in various parts of a double layer produced in a triple plasma system. A very small double plasma was used by Ripin and Stenzel [9] to excite Bernstein waves

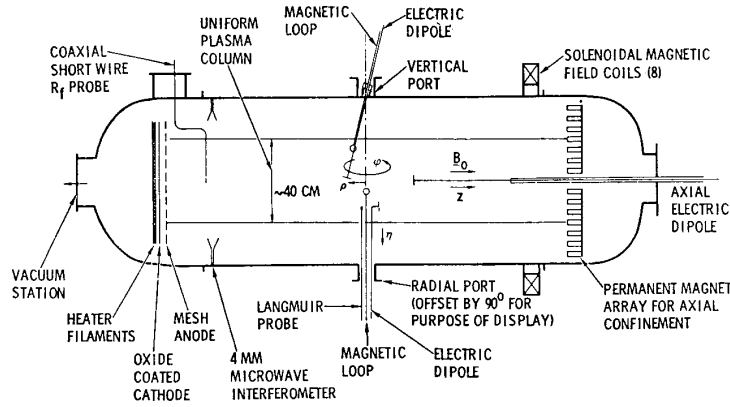


Fig. 13. Diagram of a large-area hot-cathode plasma source [10].

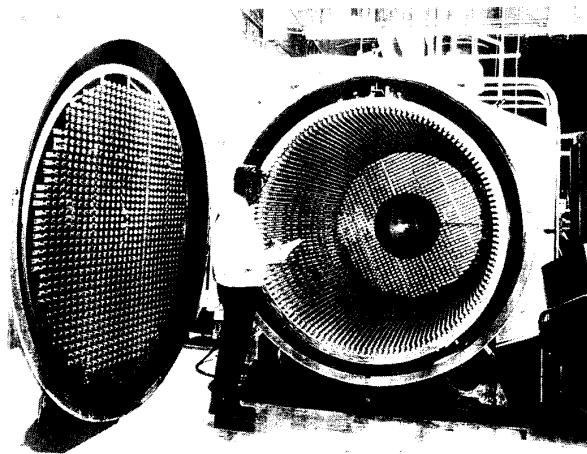


Fig. 14. A large-cathode plasma source with multidipole confinement (R. L. Stenzel, private communication).

with an ion beam. The apparatus is shown in Fig. 9, and the dispersion relation check in Fig. 10. This experiment also demonstrated the phenomenon of backward waves. Fig. 11 shows the interferometer wave pattern, which has an amplitude modulation. The wave phase velocity and the group velocity of the envelope were directly seen to move in opposite directions, in agreement with the negative slope of Fig. 10. These plasma devices have played an essential role in our understanding of basic plasma phenomena.

*D. The MacKenzie Bucket [10]*

Though not a plasma source in itself, the multi-dipole confinement scheme using permanent magnets around the surface of a plasma has improved the performance of many plasma sources by confining the primary electrons while keeping the plasma field-free in the interior. Neutral beam injectors for tokamaks, for instance, depend on this device, as do several etching and deposition tools used in the semiconductor industry. Story has it that Ken MacKenzie made the first one of these at UCLA using a surplus Navy soup pot, which not only

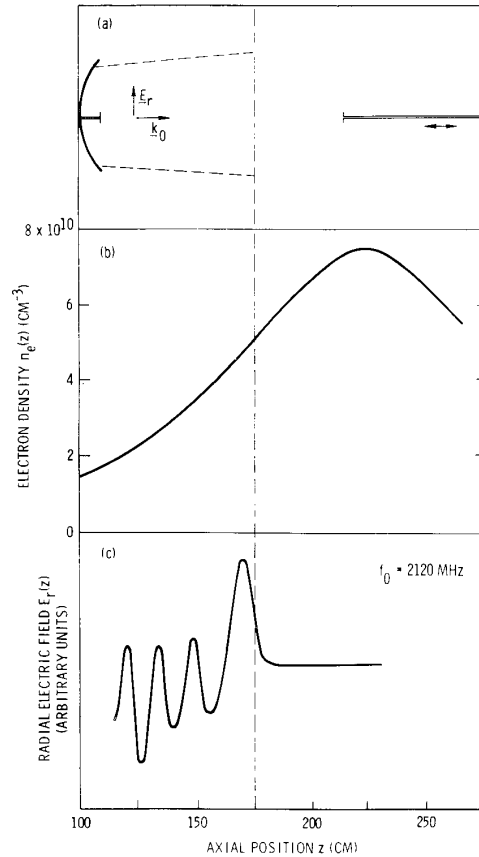


Fig. 15. Detection of Airy pattern formed by electromagnetic waves in a nonuniform plasma [11].

was made of stainless steel, but also had walls thin enough that the magnets could be put on the outside. Fig. 12 shows a modern version of the MacKenzie bucket.

*E. Large Area Cathode Discharge*

For detailed probing of a plasma, no source is better than the hot-cathode discharge developed by Stenzel [11], shown in

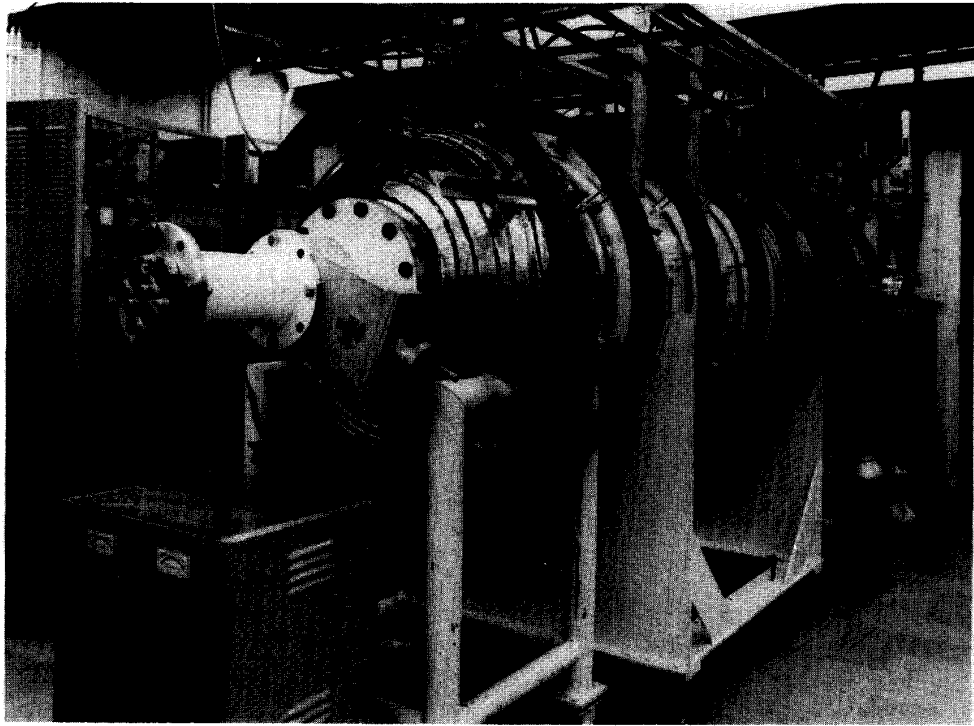


Fig. 16. A large-cathode plasma source with dc magnetic field (R. L. Stenzel, private communication).

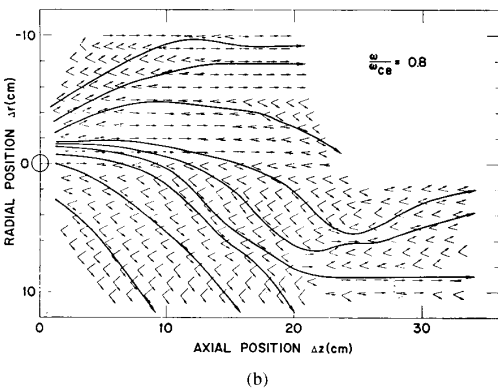
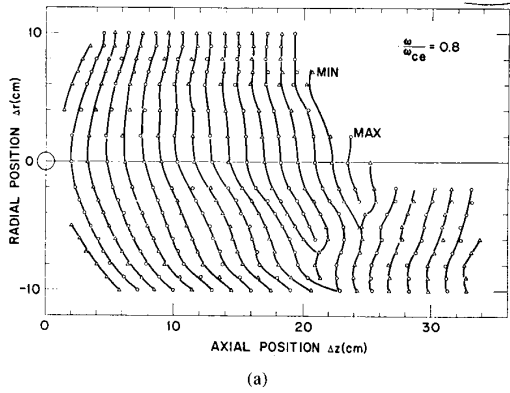


Fig. 17. Whistler wavefronts (a) and phase and group velocity directions [10].

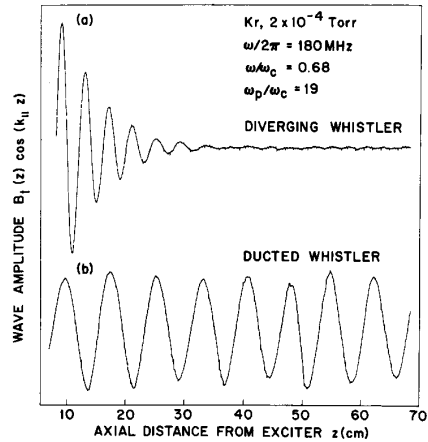


Fig. 18. Demonstration of ducted whistler waves [10].

Fig. 13. The oxide-coated cathode is stretched flat with springs and indirectly heated by filaments behind it. The emitted electrons are accelerated through a pulsed anode grid and confined radially by a weak magnetic field and axially by a multi-cusp magnet array. Stenzel and Gekelman have refined the cathode design until it can give a uniform plasma over a large volume of order 1 m diameter and 4 m long. Many probes of different varieties can be inserted without disturbing the large plasma. The magnetic field, however, is limited to about 800 G; otherwise, the plasma is subject to drift-wave instabilities when FLR or viscous stabilization is no longer

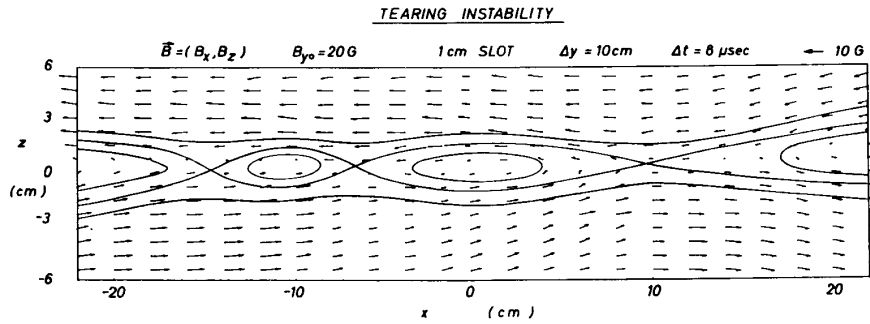


Fig. 19. Magnetic field lines in reconnection and tearing [14].

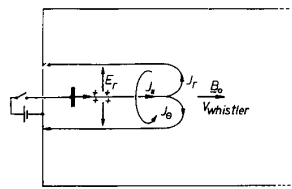


Fig. 20. Initial path of a pulsed current in a plasma [14].

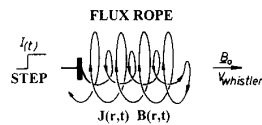


Fig. 21. Self-distortion of a current path into a flux rope [14].

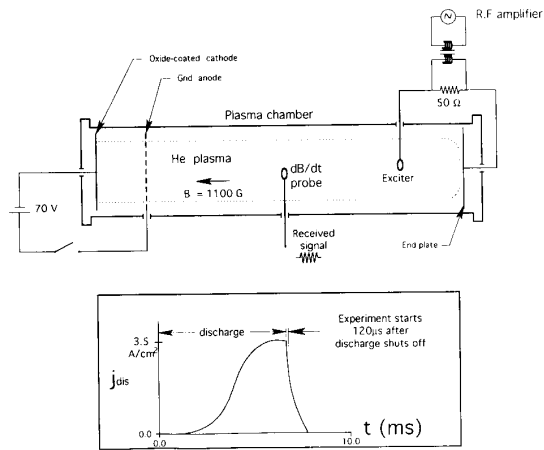


Fig. 22. Schematic of the large area plasma device [15].

effective. Fig. 14 shows the QUIPS device built at TRW, Inc.; this has multi-cusp confinement on all walls. By purposely creating an axial density gradient, Stenzel [10] demonstrated for the first time the Airy pattern that electromagnetic waves were predicted to generate when they impinge on a nonuniform plasma (Fig. 15). Stenzel's [12] investigation of whistler waves was done in another large chamber (Fig. 16) with a uniform dc magnetic field. This experiment graphically illustrated the concept of group velocity in an anisotropic medium. Fig. 17(a) shows the phase fronts of a whistler wave, laboriously mapped out with probes. At each point the phase velocity direction is perpendicular to the phase fronts, and the group velocity could be calculated theoretically from the  $\theta$  dependence of the index of refraction. The resulting arrows in Fig. 17(b) give the group velocity directions, and indeed the wave amplitude was found to maximize in the direction of energy flow. This experiment also established the space-relevant concept of nonlinear ducting, in which a wave traps itself in a density trough that it digs by its radiation pressure (Fig. 18).

Because of the large plasma volume, field annihilation could be studied in detail for the first time. Fig. 19 shows the magnetic field pattern in a tearing instability [13]. By this time data acquisition and analysis by computers had advanced so that the three-dimensional distribution functions at every point

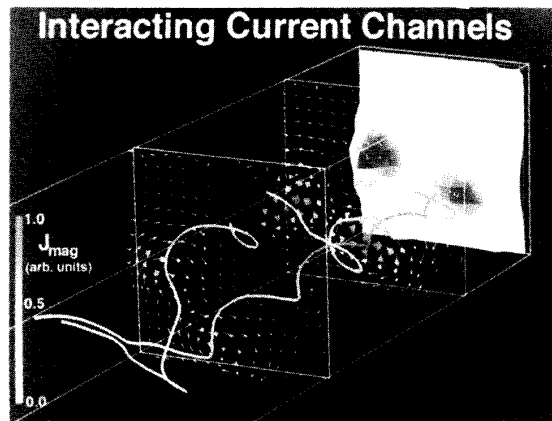


Fig. 23. Interaction of current filaments in the LAPD machine [15].

in this pattern could be measured and shown in a movie [14]. The simple conduction of current through a plasma turned out to be nontrivial. By applying a fast-rising pulse between the cathode and a collector at the far end of the discharge, Stenzel et al. [15] showed that the current flows at first backward

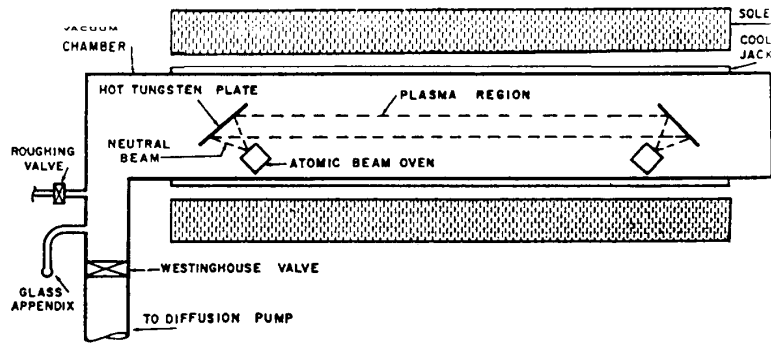


Fig. 24. Original diagram of the Q-machine [16].

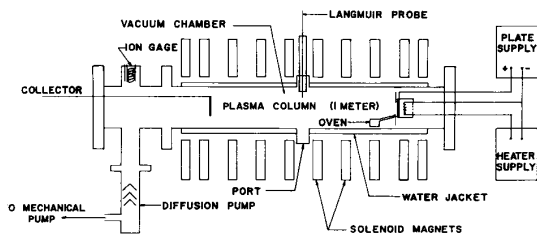


Fig. 25. Operation of a single-ended Q-machine [16].

toward the endplate, and only reaches the far end after a whistler-wave time of flight (Fig. 20(a)). The current generates its own magnetic field and falls into a force-free configuration called a flux rope (Fig. 20(b)).

Walter Gekelman has extended the large-cathode technique to even larger plasmas, using an improved cathode structure. Fig. 22 shows his LAPD device, which produces a plasma 50 cm in diameter by 10 m long in a magnetic field of up to 3 kG. With probes designed to cover the entire plasma, he has been able to simulate whistler and Alfvén wave propagation in density channels, and other phenomena such as the interaction of current filaments [16] (Fig. 23).

**F. Q-Machines**

Though it is clear that the plasma sources described above have yielded a rich variety of interesting results, perhaps the most significant and important discoveries followed the invention of the Q (for Quiescent) machine. The noise level of these plasmas was low enough that, for the first time, delicate effects like universal instabilities could be seen, and this discovery ultimately had a great influence on our understanding of anomalous diffusion. Fig. 24 is an enlargement of from the paper of Rynn and D'Angelo [17], a diagram that was a mere 1½ inches wide in the original. Fig. 25 shows how it works.

The plasma is synthesized by the injection of electrons which are thermionically emitted by tungsten "cathodes" heated to ≈2400°K by electron bombardment, and of ions which are contact-ionized from neutral beams of cesium, potassium, or barium produced in 400°C ovens. These metals

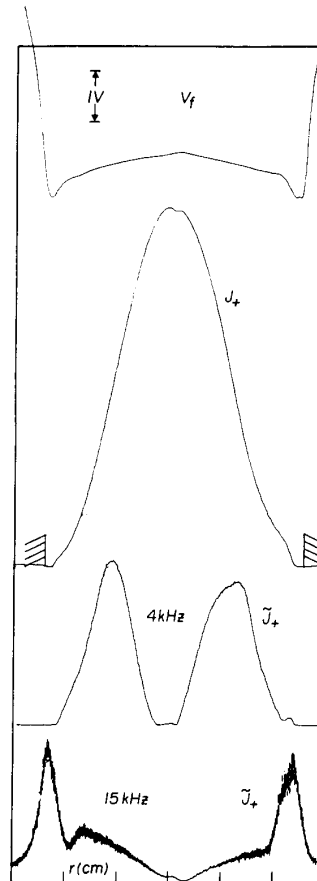


Fig. 26. Typical radial profiles of floating potential  $V_f$ , ion saturation current  $J_+$ , and drift-wave and Kelvin-Helmholtz wave amplitudes in a Q-machine.

have such low ionization potentials that when an atom impinges on a high work function material like tungsten or molybdenum, an electron is drawn into the metal, and a singly ionized ion is emitted. The plasma is held together by a strong axial magnetic field. Both species have the same temperature as the cathodes, just above 0.2 eV. Since no voltages are applied to the plasma, there are few energy



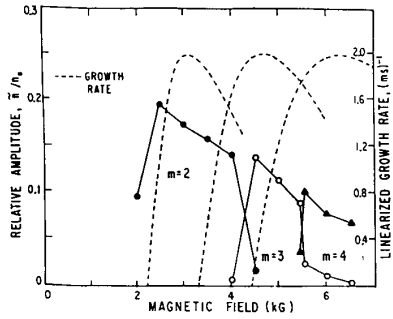


Fig. 27. Threshold behavior of drift-wave modes in a Q-machine [17].

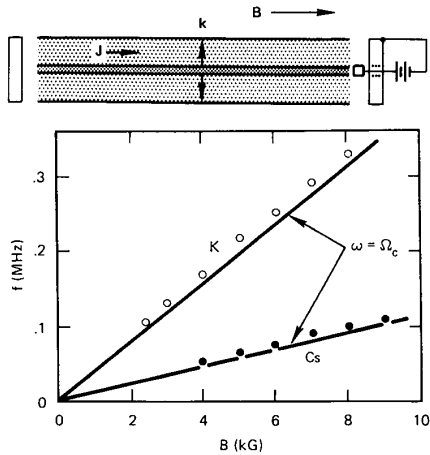


Fig. 28. Experiment for generating electrostatic ion cyclotron instability [18].

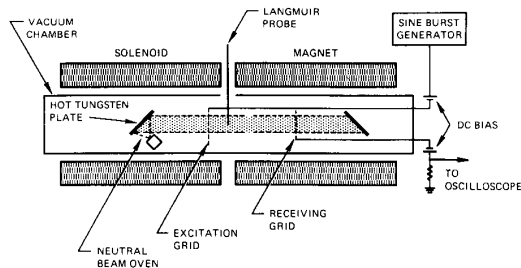


Fig. 29. Q-machine used for verification of ion acoustic waves [19].

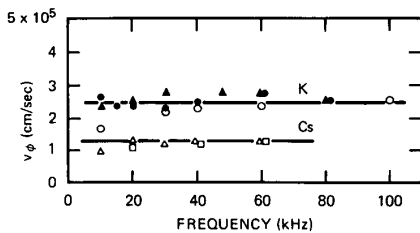


Fig. 30. Measured ion acoustic dispersion relation [19].

sources which can excite instabilities; and a quiescent plasma can be produced. Actually, there *is* an applied voltage; namely, the contact potential of several volts between the

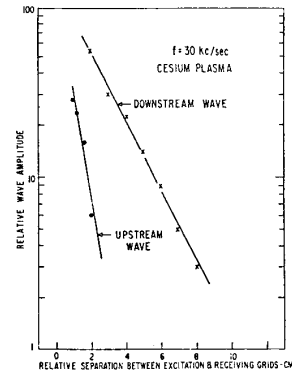


Fig. 31. Damping of ion acoustic waves [19].

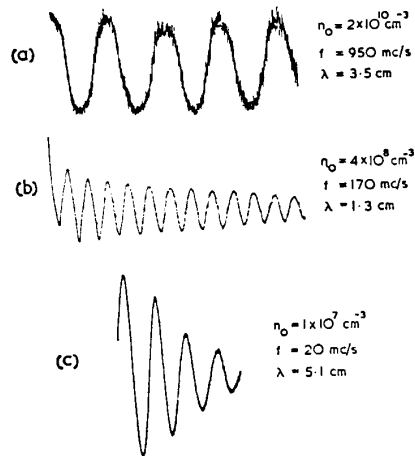


Fig. 32. Spurious electron Landau damping due to noise [20].

hot cathodes and the cold stainless steel walls, but this can be controlled by floating the vacuum chamber and applying a bias voltage  $V_c$ , as shown in Fig. 25. Fig. 26 shows radial profiles of the probe floating potential  $V_f$  and the plasma density ( $\propto J_+$ ) in a typical Q-machine. Also shown are oscillation amplitudes of noise around 4 kHz and 15 kHz when  $V_c = 0$  and the magnetic field  $B_0$  is above about 2 kG. The former peaks near the maximum of  $\nabla n$  and is due to drift waves; the latter peaks near the maximum of  $E_r$  and has been identified as a Kelvin-Helmholtz instability. Identification of the low-frequency oscillations as resistive drift waves was made by Hendel, Chu, and Politzer [18], whose famous graph showing the onset of higher azimuthal  $m$  modes with increasing  $B_0$  is shown in Fig. 27. The stability at low fields is attributed to viscous damping by the ions when their Larmor radii become large. The discovery and exploration of drift waves is perhaps the most important advance in plasma physics that is attributable to a new plasma source. Until a zeroth-order density gradient was put into the theory of plasma waves, we had no idea of why the fluctuation spectrum was peaked in the 10-kHz range

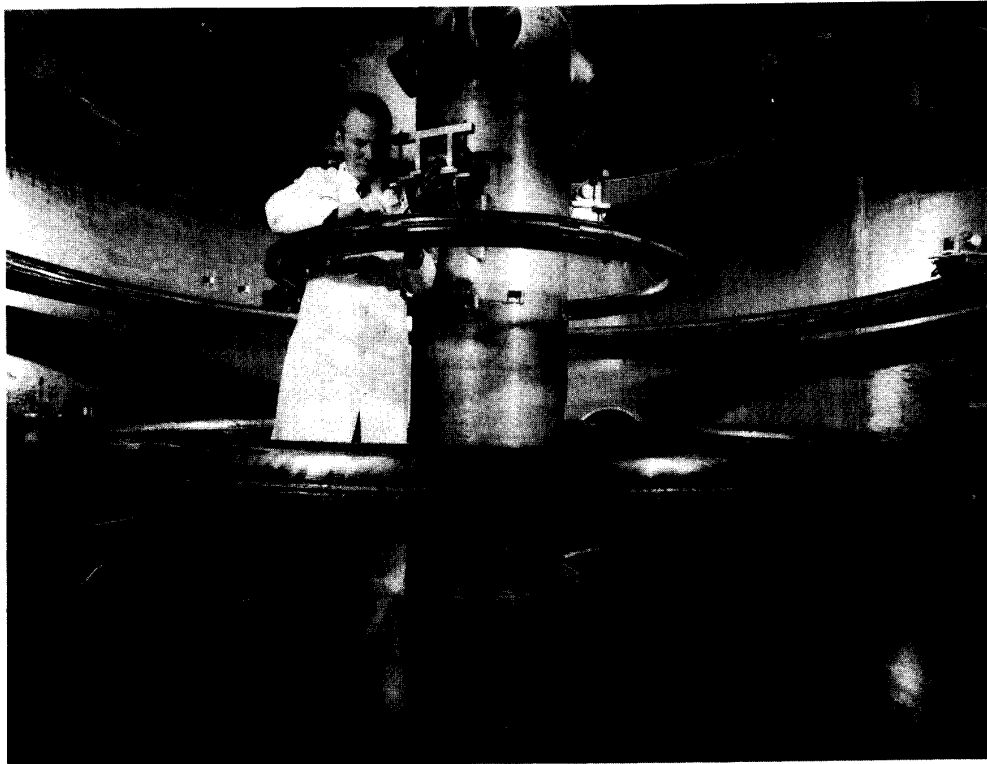


Fig. 33. The octopole machine at GA. [F. F. Chen, *Intro. to Plasma Physics*, 1st Ed. (1973).]

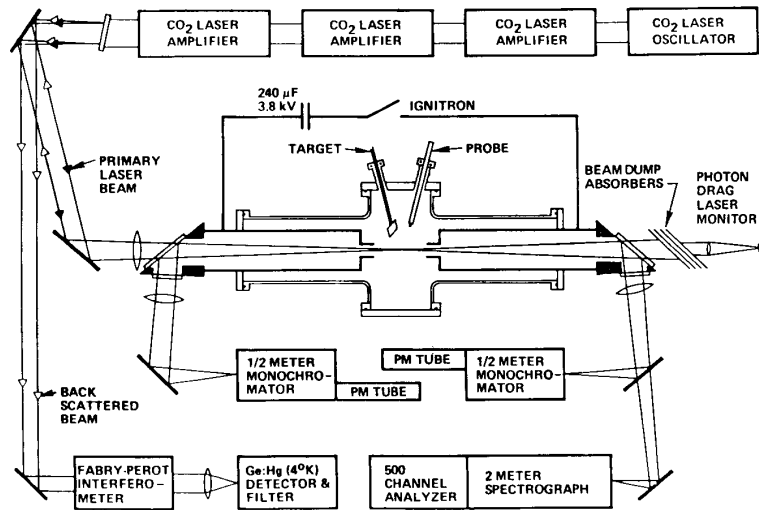


Fig. 34. High current arc used for laser-plasma interaction experiments [21].

and what it had to do with anomalous transport. Though collisionless drift waves (universal instabilities) had been found by theorists, they were buried among many predictions, most of which turned out to be unimportant in the real world. The observation of low-frequency instabilities in Q-machines, which had no source of free energy other than the pressure gradient present in any confined plasma, focused attention

on dissipative drift waves triggered by resistivity or trapped particles. Even today, 30 years after the initial excitement, drift wave turbulence is still at the forefront of tokamak confinement research.

The Q-machine also opened our eyes to other phenomena, such as electrostatic ion cyclotron waves. By drawing a current along the axis of the plasma, Motley and D'Angelo [19] saw,

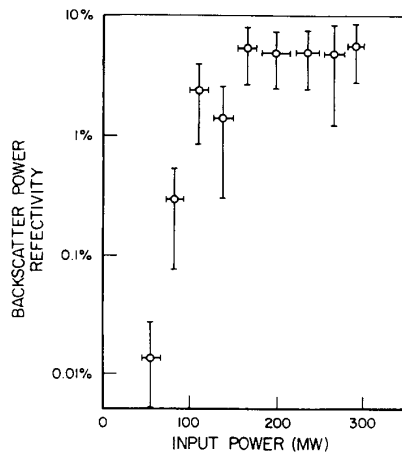


Fig. 35. Saturation level of stimulated Brillouin instability [22].

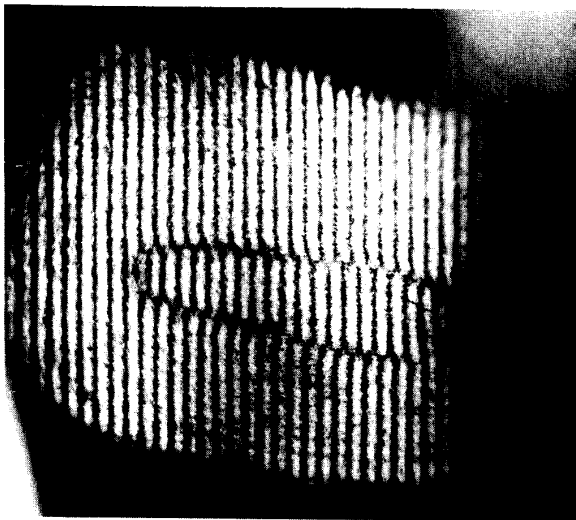


Fig. 36. Side-on interferogram showing density uniformity in laser-heated plasma [22].

for the first time, unstable waves at the ion cyclotron frequency propagating across the magnetic field (Fig. 28). This instability is important because it usually has a lower threshold than the ion acoustic instability, which theorists have studied *ad infinitum* but which is hardly ever observed.

The Q-machine also allowed Wong, Motley, and D'Angelo [20] to verify, for the first time, the existence of ion acoustic waves, which, though well known in theory, had been impossible to see in noisy plasmas. Fig. 29 shows their single-ended Q-machine, and Fig. 30 their check of the basic dispersion relation. They also measured the damping in the upstream and downstream directions, as shown in Fig. 31, thereby establishing the validity of ion Landau damping. This work actually preceded the experiment of Malmberg and Wharton, so that ion Landau damping provided our first indication that collisionless damping was real. The Malmberg-Wharton

experiment on electron Landau damping was later refined using a Q-machine by Barrett, Jones, and Franklin [21] with smaller values of  $k\lambda_D$ , where the damping was quite weak, and the damping rate was more difficult to measure. Their signals at various densities are shown in Fig. 32, where it is shown that sometimes the apparent damping is not due to Landau damping at all but to phase mixing caused by noise in Q-machines at low densities.

### G. Multipoles

Though these machines were spawned by fusion research rather than by basic plasma research, we should not leave unmentioned such devices as multipoles, spheratrons, and levitrons, which also produced quiescent plasmas. With the help of floating internal conductors, these devices could create a magnetic well and prove the principle of minimum-average-B stabilization. The two largest machines were Tihoro Ohkawa's octopole at General Atomics and Don Kerst's octopole at Wisconsin. I remember when the picture of a man standing inside the octopole (Fig. 33) was shown at the IAEA conference in Novosibirsk in 1968. The Russians were astounded that the US had the means to build a fusion machine that large, until they realized that the magnetic field was only 150G! The plasma produced was so quiescent that cross-field diffusion at the classical rate was observed here for the first time.

### H. Laser-Ionized Plasmas

The birth of parametric instabilities and laser-plasma interactions can be traced to the summer of 1973, when a surge of activity produced the main theoretical predictions on stimulated Brillouin (SBS) and Raman (SRS) instabilities. To verify these phenomena, which occurred all at once in solid targets, it was necessary to design plasma sources, used as targets, which could permit the instabilities to be observed one at a time. The critical density for a  $\text{CO}_2$  laser is  $10^{19} \text{ cm}^{-3}$ , and we needed a density that was a nonnegligible fraction of this but not as high as  $\frac{1}{4}$  of it, so as to avoid resonant layers. The first device we tried was a high-current arc, shown in Fig. 34, with holes in the anode and cathode for laser beam access. This produced densities in the  $10^{16}$ – $10^{17} \text{ cm}^{-3}$  range and permitted us [22] to observe pure SBS, uncontaminated by other effects, showing its anomalously low saturation level (Fig. 35). We found later [23] that the arc provided only part of the ionization; the laser pulse itself completed the ionization and formed a cigar-shaped region of uniform plasma, as shown in the interferogram of Fig. 36. Nonetheless, preionization by the plasma source was absolutely necessary to produce a uniform, reproducible, and jitterless plasma target.

The next problem was to isolate the SRS instability. Since SBS has a lower threshold, we had to devise a plasma source to suppress SBS. We used a slow theta pinch, shown in Fig. 37. This had good axial access; the plasma at maximum compression (Fig. 38) was uniform; the density was around  $10^{17} \text{ cm}^{-3}$ ; and, most important, the ions were hotter than the electrons, thus Landau damping the ion waves that SBS generates. This source allowed us to observe pure SRS and

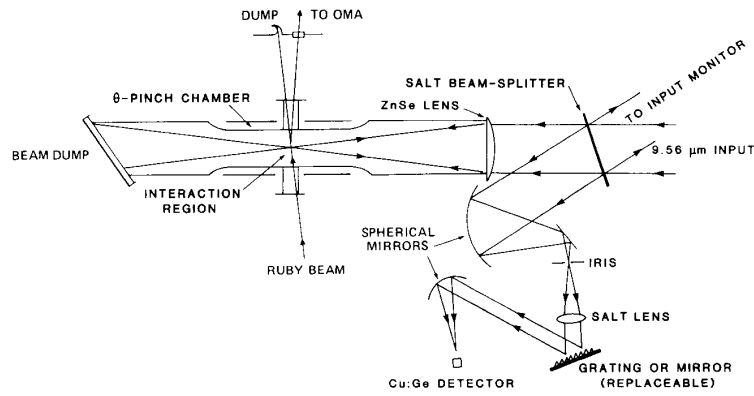


Fig. 37. Theta-pinch plasma source set up for SRS experiment [23].



Fig. 38. End-on interferogram showing density uniformity in theta-pinch plasma [23].

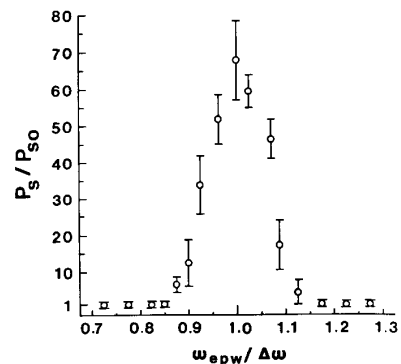


Fig. 40. Thomson scattering signal showing density resonance in beat-wave excitation [24].

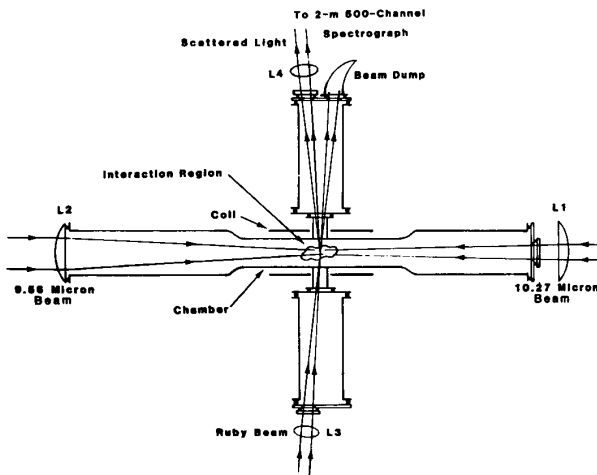


Fig. 39. Theta-pinch plasma source set up for counterstreaming beat wave experiment [24].

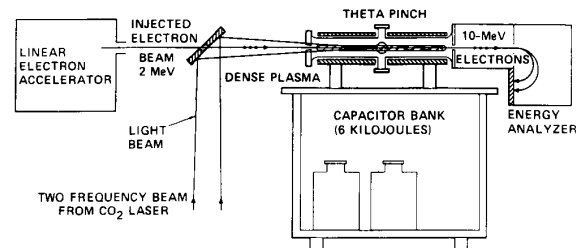
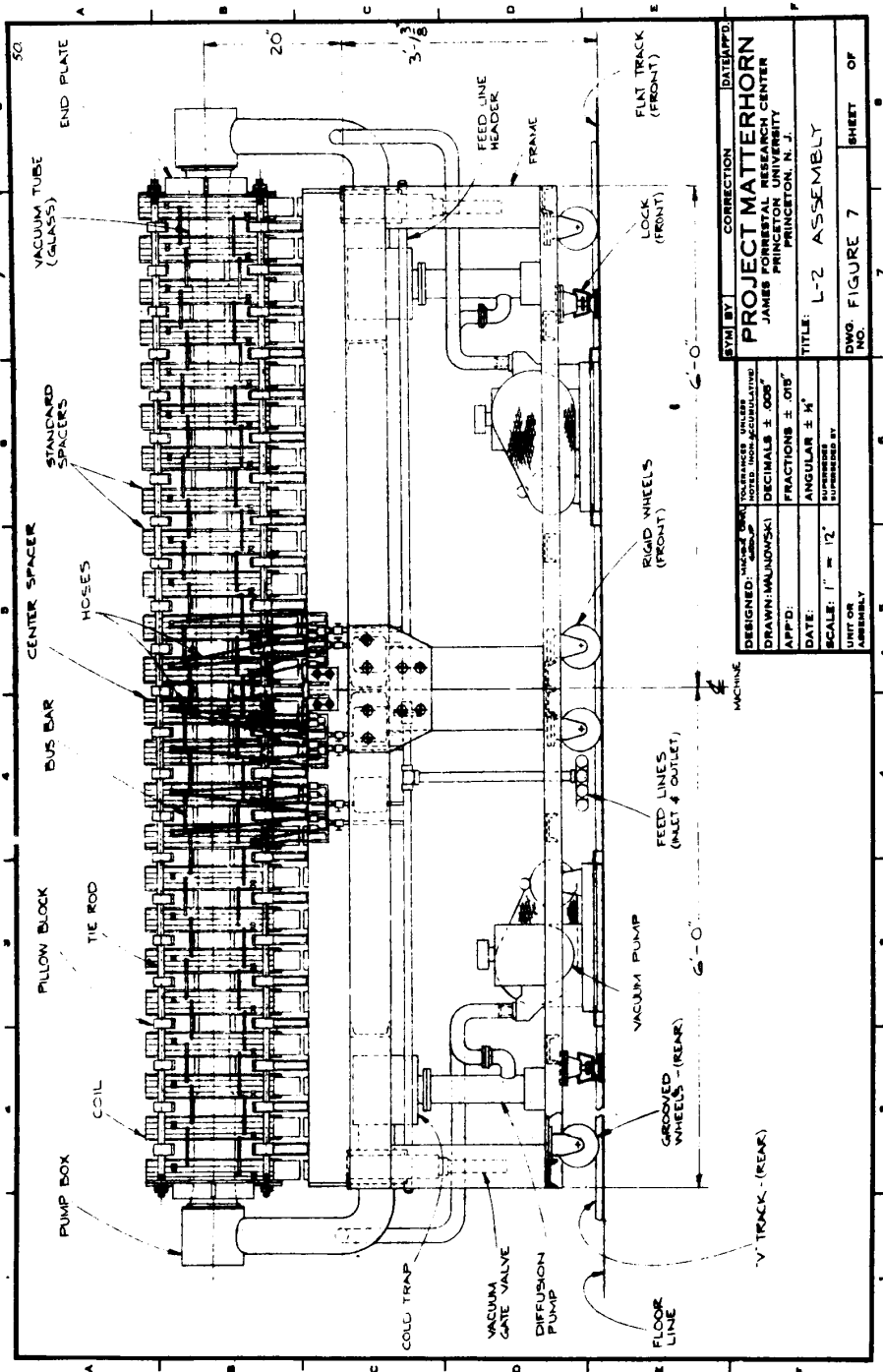


Fig. 41. Theta pinch set up for beat-wave accelerator experiment.

verify its anomalously low threshold [24]. We also used the theta pinch to demonstrate beat-wave excitation of plasma waves with counter-propagating beams [25]. Fig. 39 shows the set-up, and Fig. 40 shows the Thomson-scattering peak when the plasma frequency matched the difference frequency of the

two laser beams. Beat frequency coupling with co-propagating beams had been done on the high-current arc [26]. The theta pinch was also used initially as the plasma source for beat-wave accelerator experiments (Fig. 41). However, it turned out that small irregularities in the large magnetic field of the pinch disturbed the electron optics, and what is being used now is a small variant of the high-current arc with tunneling ionization by the laser to complete the process. The use of gas targets produced by specially designed plasma sources permitted us to check theory and find the holes in it, thus solidifying the foundations of laser interactions.



DESIGNED BY: MALINOWSKI	DATE: 1/12/72	SCALE: 1" = 12"	UNIT OR ASSEMBLY
DRAWN BY: MALINOWSKI	DATE: 1/12/72	SCALE: 1" = 12"	UNIT OR ASSEMBLY
APPROVED BY: MALINOWSKI	DATE: 1/12/72	SCALE: 1" = 12"	UNIT OR ASSEMBLY
CHECKED BY: MALINOWSKI	DATE: 1/12/72	SCALE: 1" = 12"	UNIT OR ASSEMBLY
NOTED BY: MALINOWSKI	DATE: 1/12/72	SCALE: 1" = 12"	UNIT OR ASSEMBLY
PROJECT: PROJECT MATTERHORN	DATE: 1/12/72	SCALE: 1" = 12"	UNIT OR ASSEMBLY
DESIGNER: JAMES FORNBERG	DATE: 1/12/72	SCALE: 1" = 12"	UNIT OR ASSEMBLY
DRAWN BY: MALINOWSKI	DATE: 1/12/72	SCALE: 1" = 12"	UNIT OR ASSEMBLY
CHECKED BY: MALINOWSKI	DATE: 1/12/72	SCALE: 1" = 12"	UNIT OR ASSEMBLY
APPROVED BY: MALINOWSKI	DATE: 1/12/72	SCALE: 1" = 12"	UNIT OR ASSEMBLY
CORRECTION: [REDACTED]	DATE: [REDACTED]	SCALE: 1" = 12"	UNIT OR ASSEMBLY
TITLE: L-2 ASSEMBLY		DWG. NO. FIGURE 7	
PROJECT MATTERHORN		SHEET 7 OF 7	
JAMES FORNBERG		SHEET 7 OF 7	
PRINCIPAL RESEARCH CENTER		SHEET 7 OF 7	
PRINCETON UNIVERSITY		SHEET 7 OF 7	
PRINCETON, N.J.		SHEET 7 OF 7	

Fig. 42. Design drawing of the L-2 machine [27].

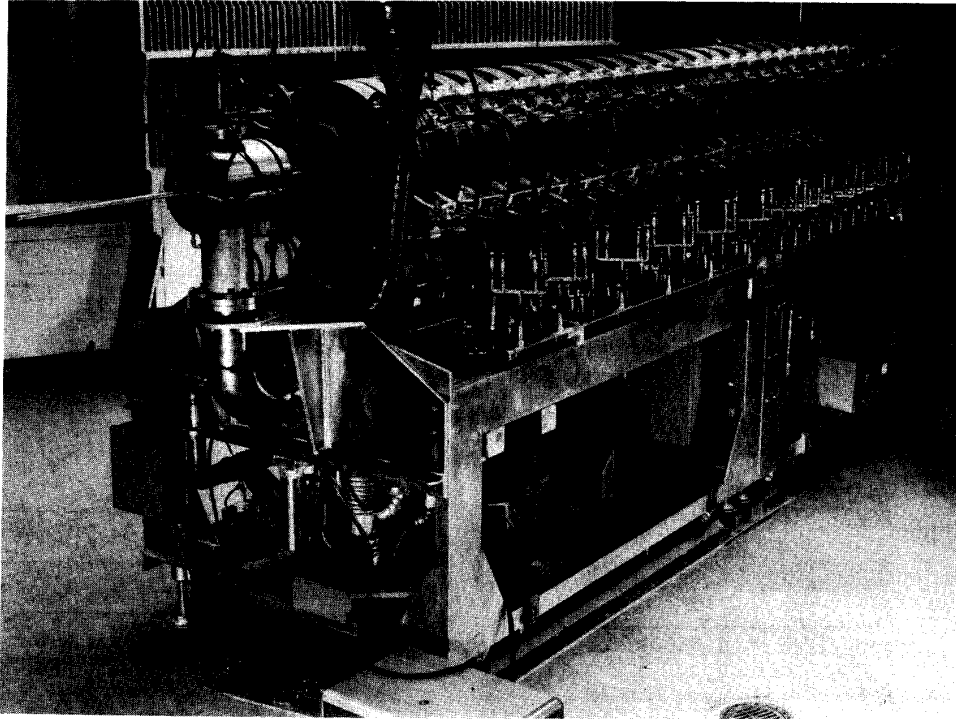


Fig. 43. The L-2 machine with the hard core installed [27].

### III. TRANSVERSE ELECTRIC FIELDS

We now move on to a group of experiments, mostly my own, which are related by a common theme: transverse electric fields. These fields have recently come into prominence because of the importance of edge layer physics in the tokamak H-mode, but the importance of transverse  $E$ -fields and my interest in them started more than 30 years ago. The H-mode itself may be considered a new break-through plasma source for investigating these fields!

#### A. The Reflex Arc

Before the invention of the Q-machine, we were searching for a plasma source that could provide a uniform, quiescent plasma in a strong, uniform magnetic field. My idea was that we had no hope of understanding anomalous transport in complicated magnetic geometries unless we first understood it in a straight geometry. The Lehnert-Hoh experiment [27] had already shown the validity of this approach, but we had to do it in a plasma that was not collision-dominated. I believe that Lyman Spitzer never forgave me for forsaking the stellarator, but at least he listened to reason and permitted me first to construct a small reflex arc L-1, and then to plan a basic research program around a large reflex arc, L-2. Fig. 42 shows an engineering drawing of L-2, and Fig. 43 a picture of it. The machine was designed by Joe File and Wendy Lehmann [28]. I understand that Joe has recently retired from Princeton; and Wendy, you may not know,

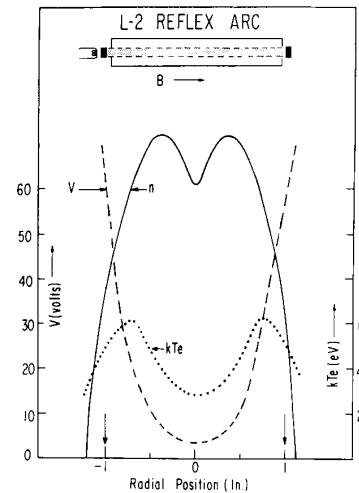


Fig. 44. Density, floating potential, and temperature profiles in the L-2 reflex arc [30].

is one of the founders of Princeton Applied Research, the makers of lock-in amplifiers that has since been absorbed by EG&G. The L-2 coil system is 12 feet long, the length dictated by the half-wavelength of Alfvén waves that we had hoped to generate at the fields and densities achievable. When the coils are arranged in groups of four, with an equal

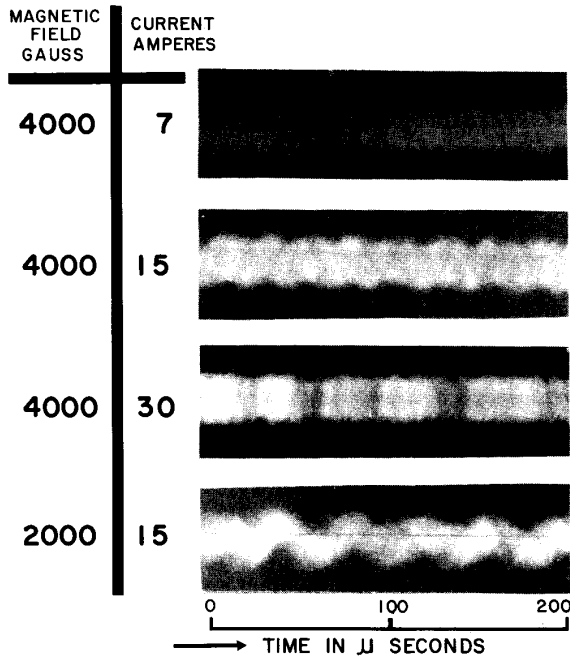


Fig. 45. Streak camera pictures of the reflex arc instability [30].

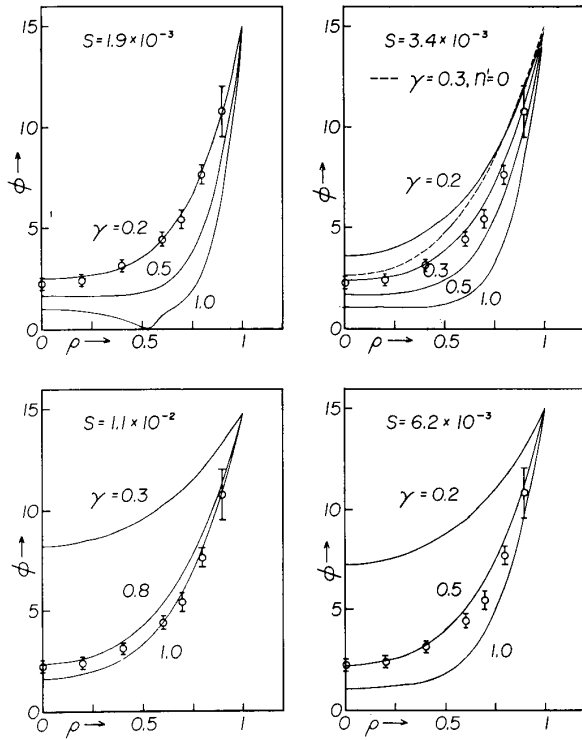


Fig. 46. Theoretical and measured potential profiles in the reflex arc [31].

length of gap for diagnostic access, the maximum field is 4 kG. The machine was later converted into a Q-machine

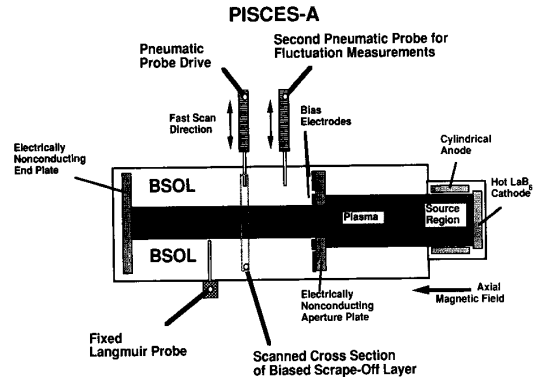


Fig. 47. The PISCES-A reflex arc [32].

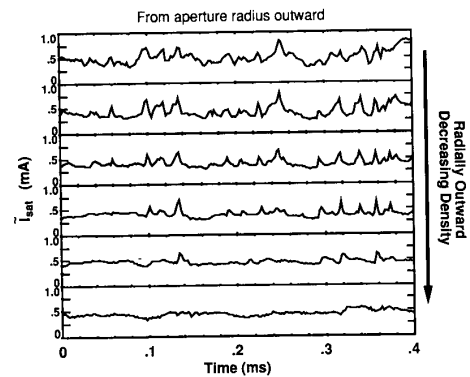


Fig. 48. Fluctuation level in the PISCES-A reflex arc [32].

and then dismantled after 1969. The L-2 coils, however, seem to have a life of their own and will probably outlive all of us. First used at Princeton for the ACT-1 machine, the coils are now dispersed all over the country, serving experiments at Brookhaven, North Carolina, Wisconsin, and UCLA Physics.

The L-2 reflex arc used hot cathodes, four-inch diam slabs of tungsten heated by electron bombardment to 2400°K. The filaments emitting the bombardment current were pre-bent in the direction of the  $\mathbf{j} \times \mathbf{B}$  force so as to maintain their shape at all magnetic fields [29]. The two cathodes are connected together and biased negatively relative to the main chamber (the anode), which was at ground. This caused the discharge current to flow across the strong magnetic field to the anode. The primary electrons emitted from the cathodes were confined longitudinally by the electrostatic sheaths at each end and therefore permitted higher ionization efficiency than in a straight arc. The density, temperature, and potential profiles shown in Fig. 44 indicate a fairly uniform plasma suitable for experiments, but the plasma was subject to a high level of turbulence, as shown by the streak camera pictures of Fig. 45. The cause of the noise was not known at the time, but it is clear that such reflex discharges cannot possibly work without some sort of anomalous diffusion, since the electrons carrying

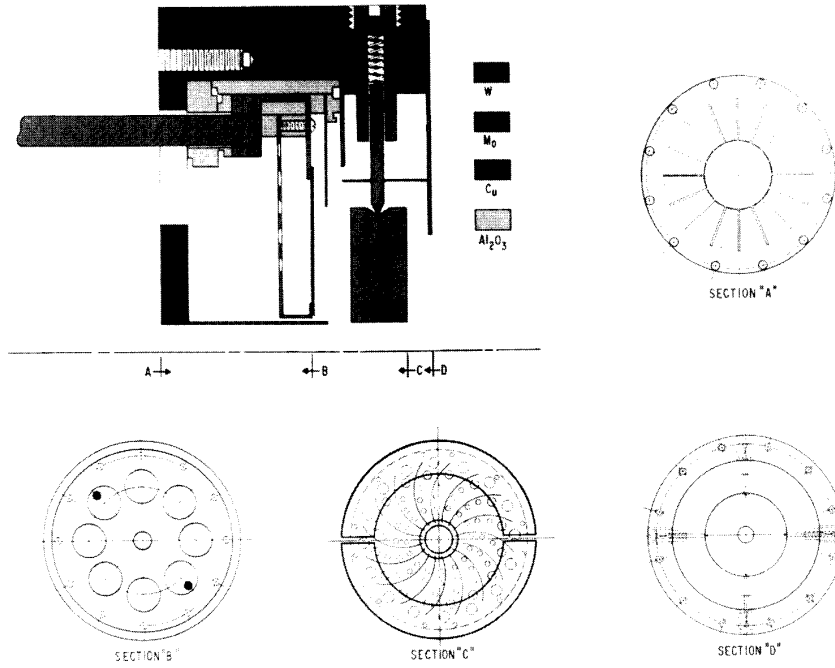


Fig. 49. Cross section of cathode structure with insulated aperture limiter and hole for hard core.

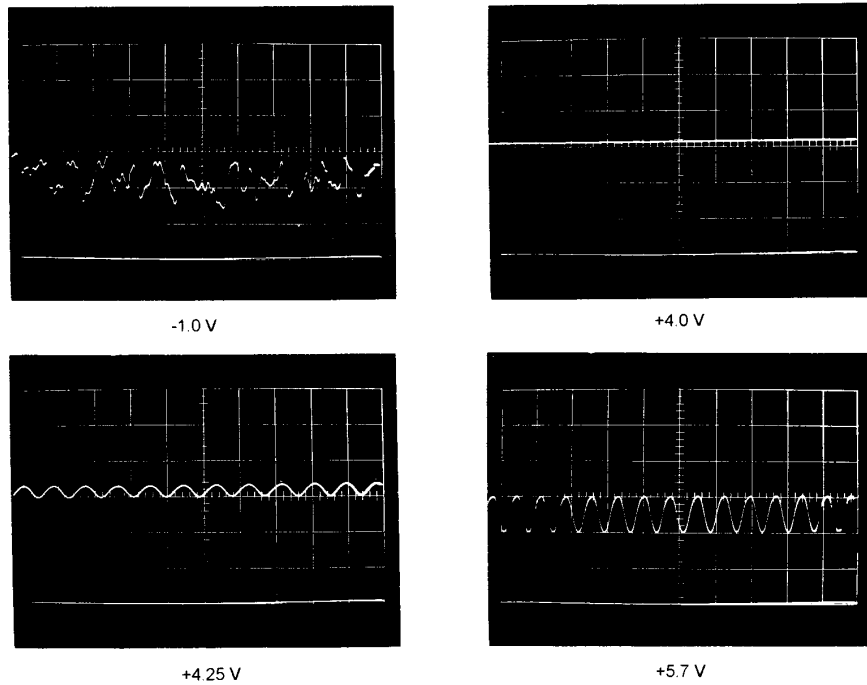


Fig. 50. DC coupled saturation ion probe current showing onset of drift waves as limiter bias is varied [34].

the discharge current in such reflex or PIG (Phillips Ionization Gauge) discharges must cross the magnetic field to reach the anode. That the inward radial electric field excites a strong  $E \times B$  instability in a partially ionized plasma was later pointed out by Al Simon [30], but the theory came too late. The basic

experiments that were planned could not be carried out, and two years of data on the operation of the discharge could not be explained, and therefore could not be published except in preliminary reports [31]. By the time theoretical understanding of the  $E \times B$  instability enabled us to design a discharge that



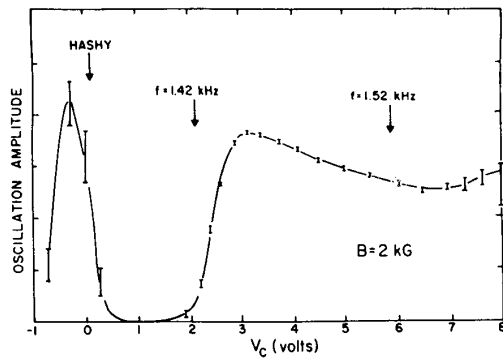


Fig. 51. Drift wave amplitude versus limiter bias  $V_c$  [34], [35].

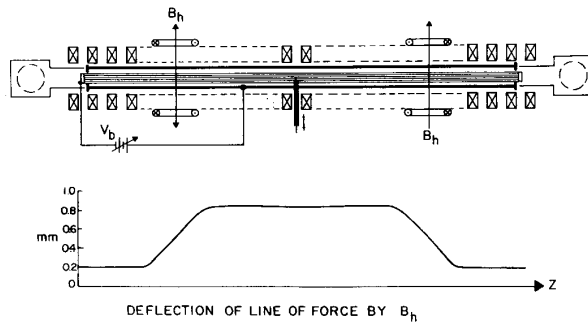


Fig. 52. Vertical field coil system used to displace the plasma [35a].

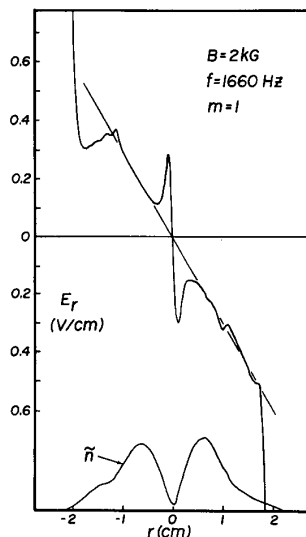


Fig. 53. Radial electric field profile measured with oscillating plasma [36].

would be free of it, the Q-machine had been invented, and there was no longer a need to do so.

However, all was not lost. By assuming a Bohm diffusion rate, we could solve the discharge balance equations and predict the observed radial potential profile, as shown in Fig. 46 [32]. This much understanding was sufficient for PMT, Inc. to manufacture a reflex arc source for optical coatings, and

for Bob Conn's group to use the reflex arc as a high-density source for the PISCES program. Fig. 47 shows a diagram of PISCES -A and Fig. 48 the oscillation level in it [33]. When used for testing fusion materials and divertor designs, the basic instability of the plasma is of little importance. When used for studies of edge-layer physics, however, the PISCES machines would benefit by replacement of the reflex arc by a more stable source, such as the helicon source we will mention later.

The L-2 machine was also used for an experiment on beam-plasma interactions. A 2-A, 20-kV electron beam from a Varian microwave tube was injected through a hole in one of the cathodes. Though many interesting effects were observed [34], none of them agreed with any known theory. Again, we were ahead of our time. I learned an early lesson in that experiment which I convey yearly to my students: Always learn to walk before trying to run. I should have started with a weak beam and worked near the threshold.

### B. Edge Stabilization of Drift Waves

Converting the L-2 reflex arc into a Q-machine was relatively simple, since we already had hot cathodes. We changed from 4 in diam, 0.25 in thick tungsten plates to 2 in diam, 0.5" thick ones in order to have a more uniform surface temperature, and hence a more uniform potential distribution in the plasma. There were three large Q-machines operating at Princeton at the time, but a number of experiments were particular to the L-2Q device. By installing an insulated aperture limiter in front of the cathodes, as in Fig. 49 [28], we were able to see the effect of applying different potentials  $V_c$  to the edge of the plasma. We found we could stabilize and destabilize drift waves this way. Fig. 50 shows the dc coupled probe current versus time for various bias voltages. Below +4 V, there was a turbulent spectrum of drift waves. At 4.0 V, the plasma suddenly became completely quiet. As  $V_c$  was slightly increased, sinusoidal drift waves could be seen and studied at threshold. The waves grew with increasing bias, and eventually became nonlinear. The amplitude behavior with  $V_c$  given in Fig. 51 [35]. There is a 2-V range of edge biases in which the drift waves are stabilized.

This observation was a clear indication of the strong effect of electric field shear on plasma stability. The problem was to prove it definitively. The first step was to measure the radial electric field accurately. If one were to take radial profiles of floating potential, one would have to take the first derivative to get  $E_r$ , the second derivative to get  $E'_r$ , and the third derivative to get  $E''_r$ , these terms being important in the Kelvin-Helmholtz effect. It would be much better to measure  $E_r$  directly. We could do this by making a vibrating probe, which would continuously measure the potential difference at two radii separated by, say, 1 mm. However, the design and construction of such a probe would have taken the Princeton engineers months, and there was also the danger that vibrations in the connecting cable could generate electrostatic charges. I decided to vibrate the plasma instead. This could be done by adding two sets of coils producing a vertical  $B$ -field, as

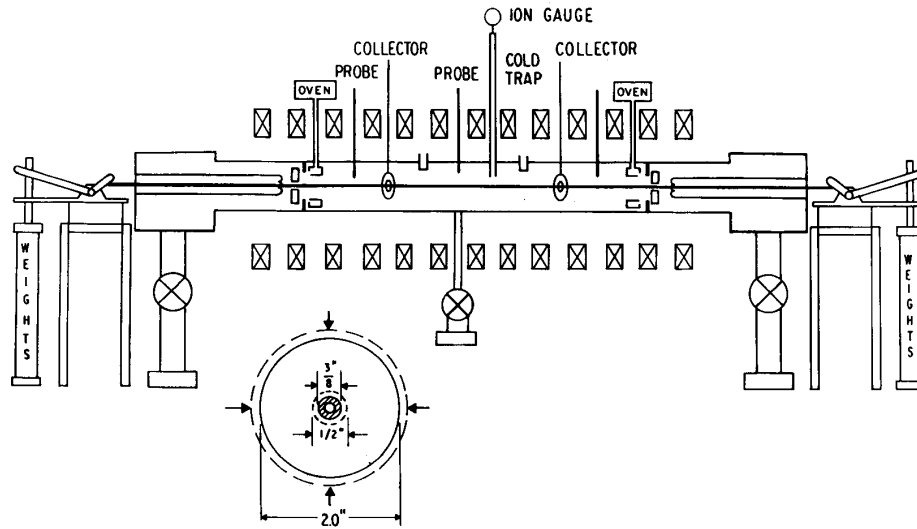


Fig. 54. Diagram of L-2 Q-machine with hard core.

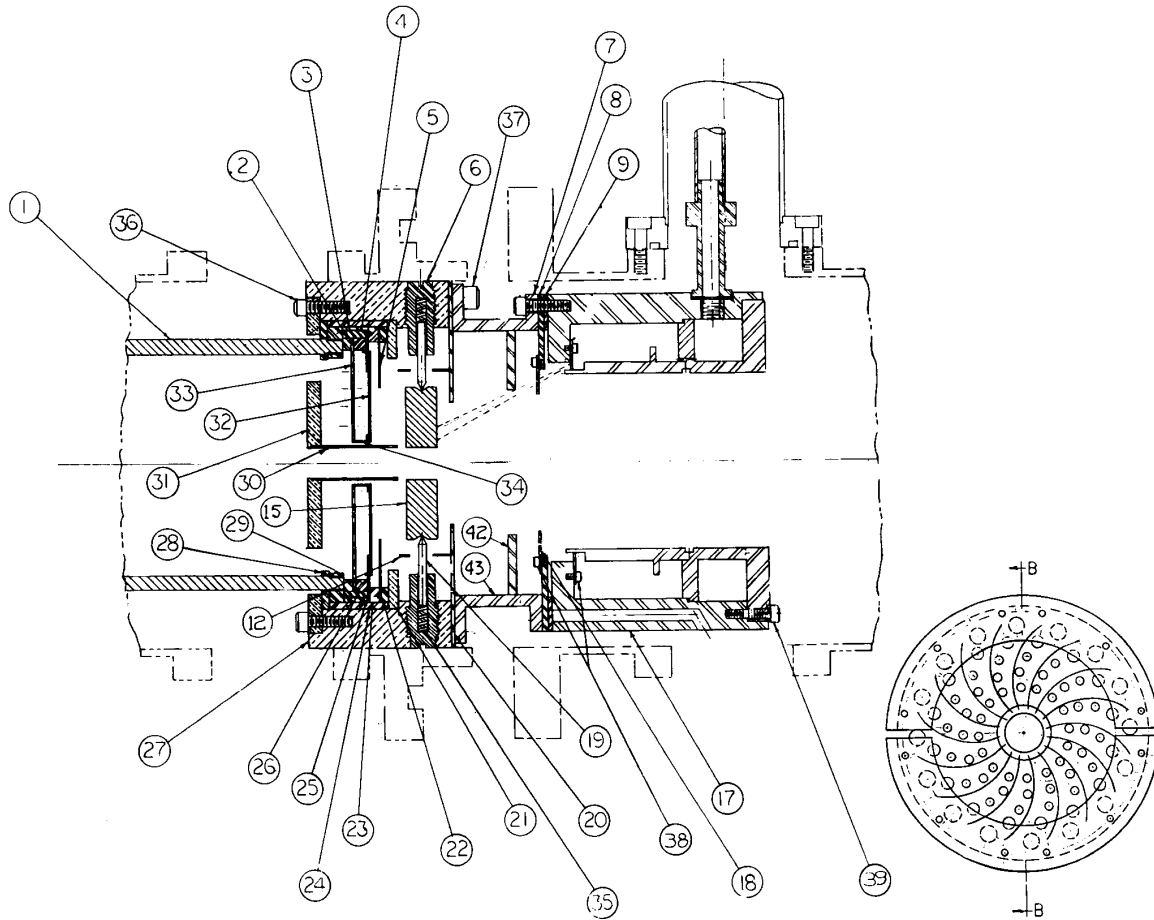


Fig. 55. Modified cathode assembly with hard core feedthrough on axis.

shown in Fig. 52. By applying a 10-Hz sine wave to these coils, the plasma was moved up and down uniformly by a few

mm at that frequency, and a lock-in amplifier tuned to the 10-Hz signal directly gave the electric field at the probe location.

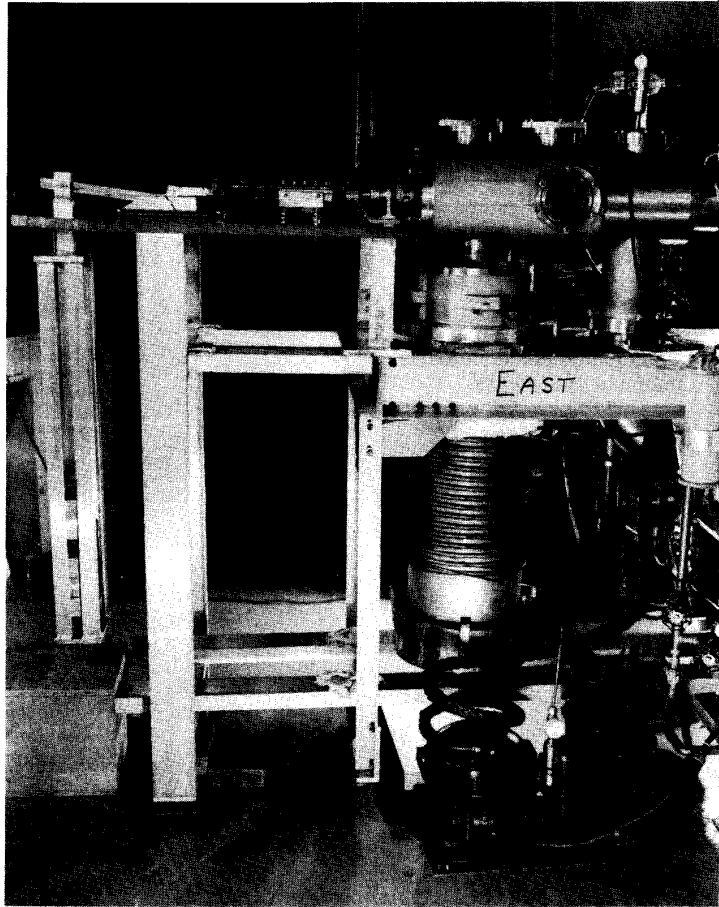


Fig. 56. Cantilever system for keeping hard core straight.

The frequency was chosen to be low enough to avoid exciting ion acoustic waves, but high enough to be usable with a lock-in amplifier. The coils, made of house wiring, were wound in one afternoon on wooden forms, and they were driven by two hi-fi amplifiers (stereo had not yet been commercialized).

The whole setup was done in one day, and the experiment worked like a dream. A typical electric field profile is shown in Fig. 53 [36]. The wiggles near the axis were due to the hard core we had in the machine at the time (to be described in the next section), and the large  $E$ -field at the edge is due to the contact potential between the hot tungsten cathodes and the cold aperture limiter. In the body of the plasma, the  $E$ -field is linear with radius, corresponding to rigid-body  $\mathbf{E} \times \mathbf{B}$  rotation of the plasma. *There was no noticeable change with limiter bias*, even though the oscillation amplitude varied wildly. Whatever was happening at the extreme edge we could not see accurately enough, but the electric shear at the maximum of the density gradient did not seem to be affected. This was a disappointing negative result, but we thought that at least the measurement technique was worth publishing. There is an interesting story behind why it was never published. Ken Rogers and I were working on this during his sabbatical, and

he was put in charge of submitting this particular paper to Rev. Sci. Instrum. and seeing it through the refereeing process. Soon thereafter, he was made President of Stevens Institute of Technology. When the paper came back from the referee, it never saw the light of day in his office. So I have learned one thing about college presidents. They could care less about publishing another paper.

### C. Shear Stabilization of Drift Waves

Since we had a source of drift waves that was under control, it was natural to see how they could be stabilized by  $\min\text{-}\mathbf{B}$  and by shear. Let us consider the shear experiment. To impose magnetic shear, we decided to make 0.5 in holes in the cathode and filament assemblies and to string a water-cooled conductor through the holes to generate a  $B_\theta$  field. When this problem was given to the engineers, they came up with the following solution: The hard core would be an aluminum tube, which had a better combination of weight and conductivity than copper, and there would have to be a cantilever system with lead weights to keep the tube straight as it heated and expanded during the current pulse. Diagrams of the setup and the modified cathode as-

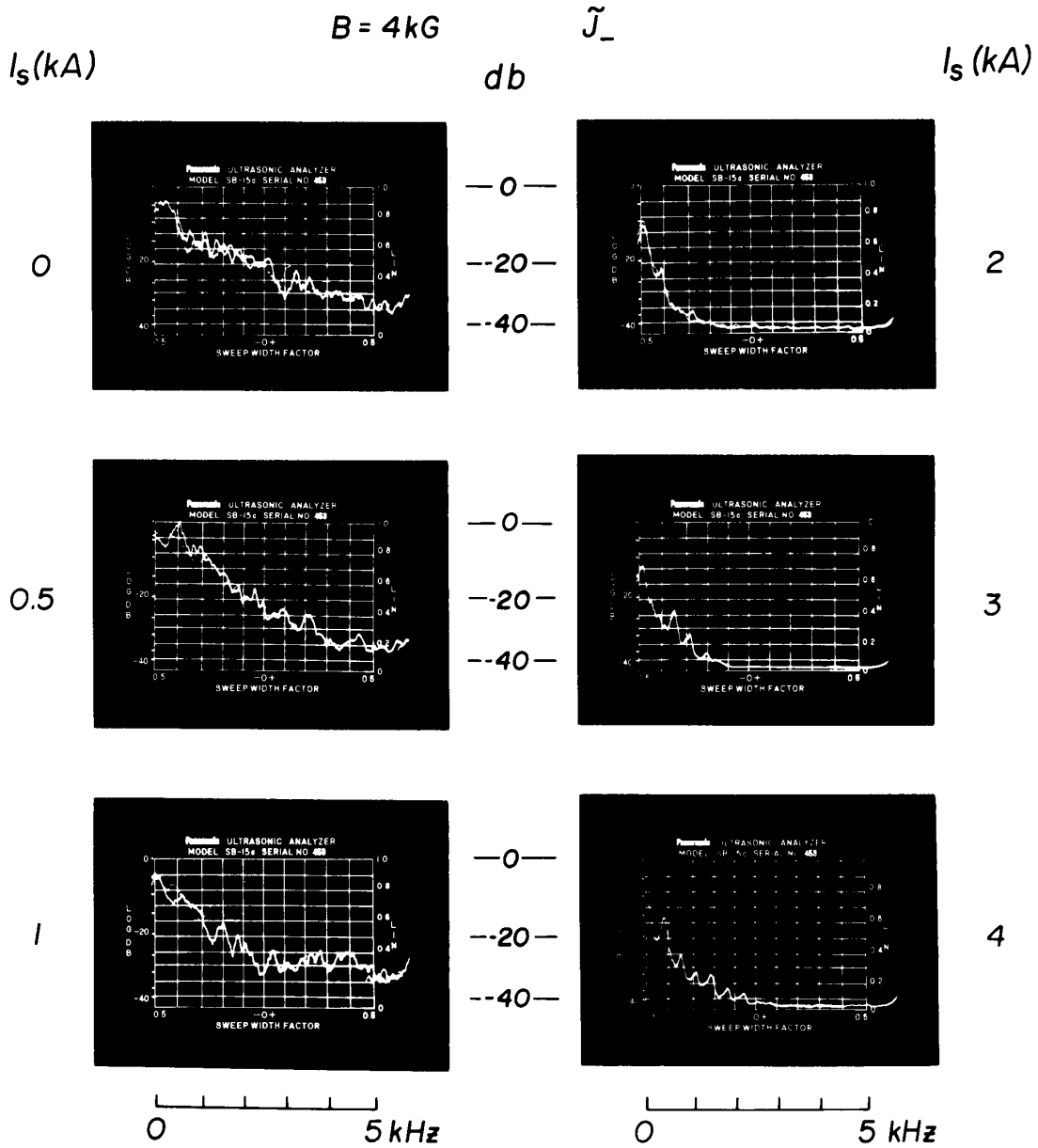


Fig. 57. Change of drift wave spectrum with hard core current [35b].

sembly are shown in Figs. 54 and 55, and a photograph of the cantilever system is given in Fig. 56. When the hard core was pulsed, the lead weights sank; and after the pulse, they came back up. It was truly a Rube Goldberg device, but it worked. I think the physicists and the engineers at Princeton were amused at each other—the engineers that the physicists would want to do something like this, and the physicists that the engineers would come up with such a solution. The clearance between the hot tungsten cathodes and the water-cooled aluminum hard core was only about 0.5 mm, so this was an accident waiting to happen . . . and

it did. However, we recovered in time to make the APS deadline.

Fig. 57 shows the drift wave spectrum for various values of the current  $I_s$  in the hard core. It is clear that 2 kA of current greatly reduced the drift wave turbulence. To see how the shear stabilization actually worked, my first student, Dave Mosher, probed the floating potential over a cross section of the plasma [35]. He found that the application of shear produced ripples whose wavelength decreased with increasing shear, as shown in Fig. 58. What was happening was that small temperature variations over the cathodes produced asymmetric

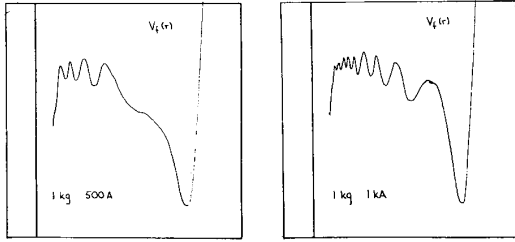


Fig. 58. Spatial oscillations in plasma potential in the presence of shear [34], [36].

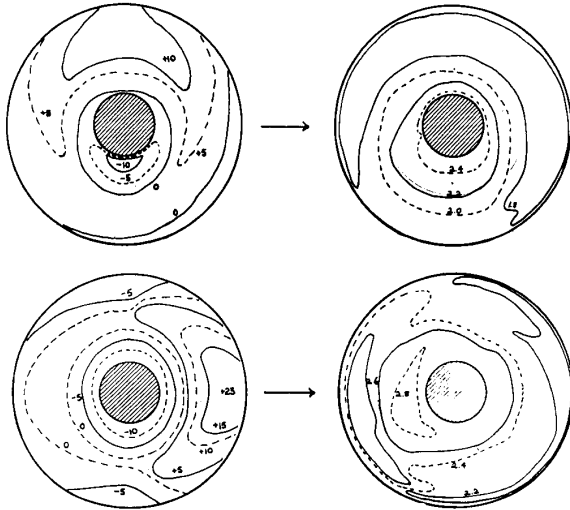


Fig. 59. Asymmetric isopotentials in plasma caused by temperature nonuniformities in cathode.

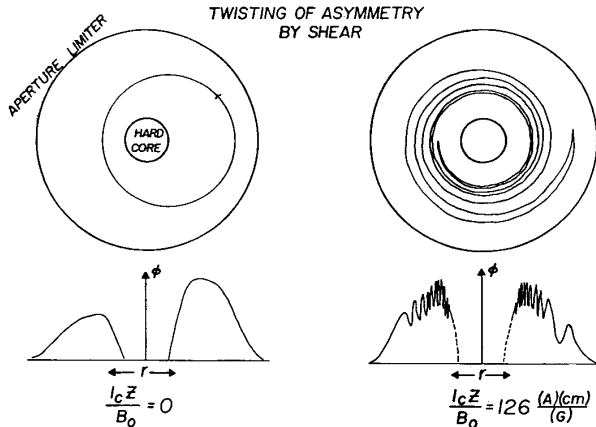


Fig. 60. Equipotential contours twisted by magnetic shear, providing the mechanism of shear stabilization [34], [35a], [35b].

potential contours in the plasma, giving rise to convective cells (Fig. 59). Plasma would  $E \times B$  drift along these isopotentials and reach large radii rapidly. When the magnetic field lines are twisted by shear, these isopotentials are twisted into

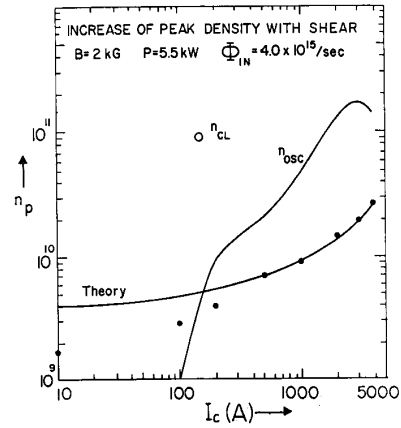


Fig. 61. Increase of plasma density with hard core current. The theoretical curve is based on the twisting of the equipotentials. The point  $n_{cl}$  indicates the density there would be if transport were classical. The curve  $n_{osc}$  indicates the density there would be if all transport were due to oscillations; the measured oscillation amplitude is used [34], [35a], [35b].

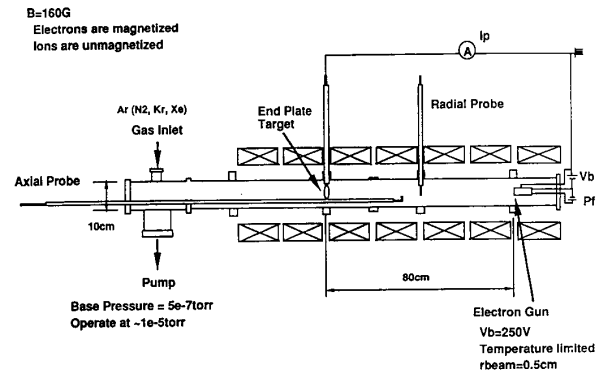


Fig. 62. Apparatus for weak beam-plasma experiment [36].

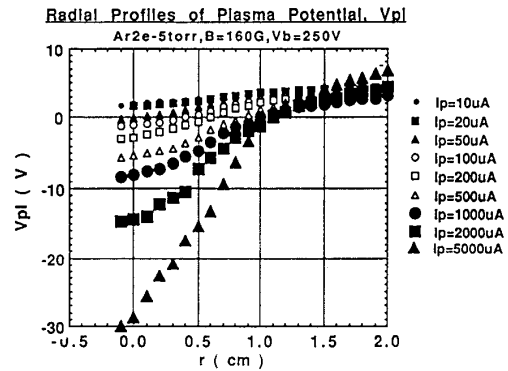


Fig. 63. Potential profiles measured in weak beam-plasma experiment [36].

long spirals, shown in Fig. 60, which manifest themselves in the observed ripples. The twisting has the double effect of suppressing drift waves by squeezing them into a band narrow enough that ion viscous damping can be effective, and

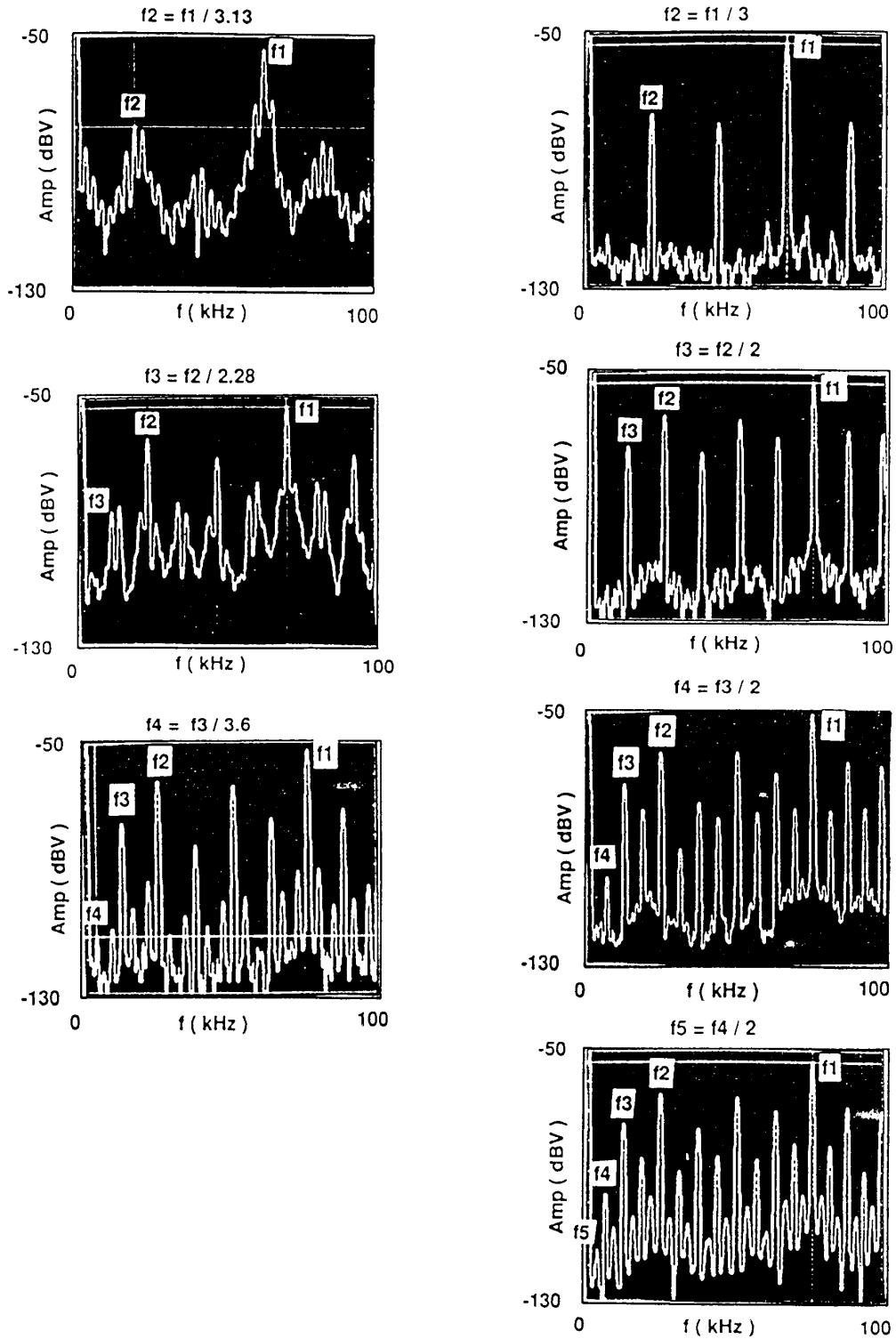


Fig. 64. Unstable oscillations generated by electron beam [37].

of increasing the length over which plasma must drift before reaching the outside. Indeed, the plasma density measured at the highest shear was about half of that expected from purely

classical diffusion (Fig. 61). Note in Fig. 61 the curve labeled  $n_{osc}$ . This is the density that would be expected if all transport is by oscillatory diffusion. When the drift wave

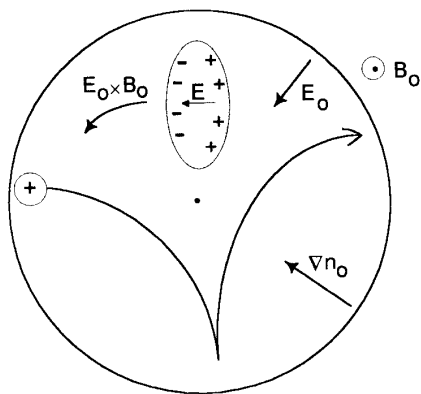


Fig. 65. Mechanism of the modified  $E \times B$  instability. The  $E \times B$  rotation of the ions is much smaller than of the electrons, causing a charge separation wherever there is a positive density fluctuation. The resulting first-order  $E$ -field causes an outward drift when  $E_0$  and  $\nabla n_0$  are both inward. This drift increases the local density at the expense of  $\nabla n_0$ .

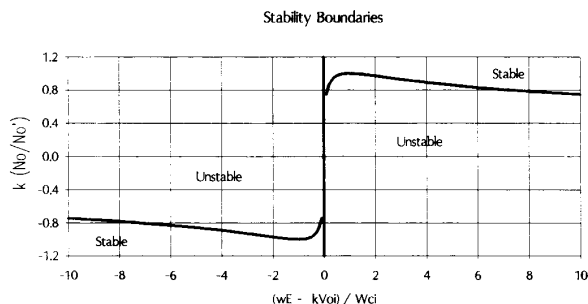


Fig. 66. Stability boundaries of the collisionless  $E \times B$  instability with large ion orbits [39].

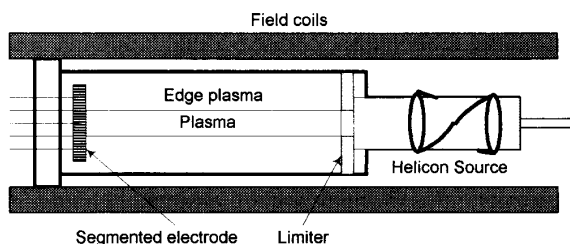


Fig. 67. Conceptual experiment using a helicon source to study tokamak edge layer physics.

amplitude is greatly reduced by shear, the expected density is much larger than that observed, showing that most of the remaining loss is by convection rather than oscillatory diffusion.

*D. E x B Instability in a Beam-Created Plasma*

We have seen that a transverse electric field of the right sign can excite the reflex-arc instability in a partially ionized plasma. The instability mechanism depends on the charge separation arising when the ions and electrons do not have

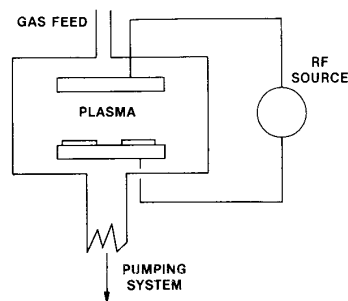


Fig. 68. Schematic of a parallel-plate capacitive discharge [40].

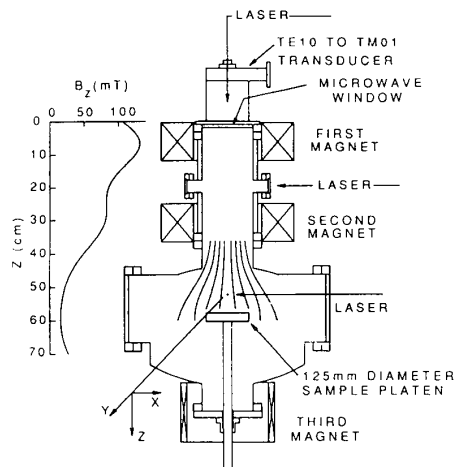


Fig. 69. Schematic of an electron cyclotron resonance source [41].

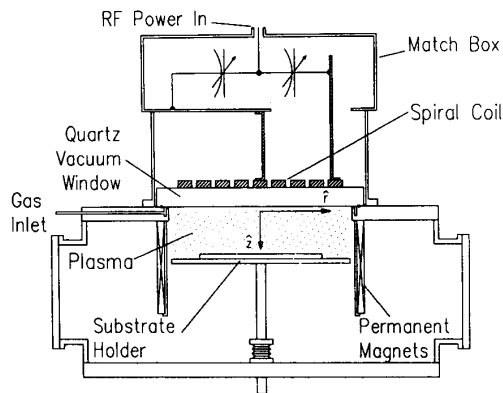


Fig. 70. Schematic of an RFI or TCP plasma source [42].

identical  $E \times B$  drifts because of the neutral drag on the ions. In fully ionized plasmas a small finite-Larmor-radius effect can cause drift-wave-like instabilities, but only when  $k_{||}$  is finite. However, in weak magnetic fields in which the electrons are magnetized but the ions have Larmor orbits much larger than the plasma, the charge separation is so strong that even flute instabilities with  $k_{||} = 0$  can arise. This instability

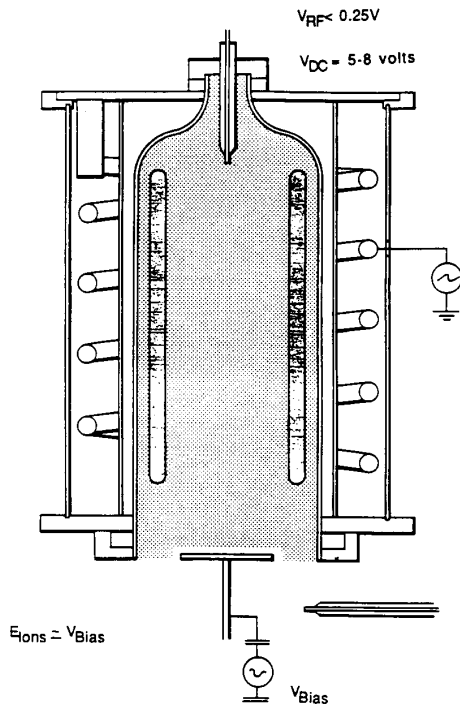


Fig. 71. Schematic of an inductively coupled discharge [43].

was discovered in the course of an experiment on chaos by Sakawa [37] as part of his Ph.D. dissertation at UCLA. Fig. 62 shows the apparatus. In a uniform 160-G magnetic field, a weak electron beam ( $100 \mu\text{A}$  at 250 V) is injected into  $2 \times 10^{-5}$  Torr of argon, ionizing a tenuous plasma of order  $10^7$ – $10^8 \text{ cm}^{-3}$  in density. The negative charge of the beam causes a radial electric field of the proper sign for instability, as shown by the potential profiles of Fig. 63 for various beam currents. Oscillations of two or more frequencies are seen; these are shown in Fig. 64 to lock into each other when they are harmonically related and generate turbulence through mode-coupling [38]. We are interested here in what causes the instability in the first place. The fundamental frequency is higher than the ion cyclotron frequency and much lower than the diamagnetic drift and  $\mathbf{E} \times \mathbf{B}$  frequencies, thus eliminating all previously known instabilities. Here the small-but-finite ion Larmor radius picture is not at all appropriate, since the ions bounce in the radial potential well with orbits that are barely curved by the  $\mathbf{v} \times \mathbf{B}$  force, as shown in Fig. 65. The finite curvature is all-important, because it causes a slow azimuthal drift of the ions, and this drift frequency is the only frequency that agrees with the observed one. By treating the ion orbits without a small-FLR expansion, we have found [39], [40] that indeed there should be a large growth rate in the experiment, and that the region of instability (Fig. 66) covers all but the weakest electric fields. This instability may be important in the weak-field discharges used in plasma processing and in strong electric field layers whose scale length is comparable to or smaller than the ion Larmor radius at the electron temperature.

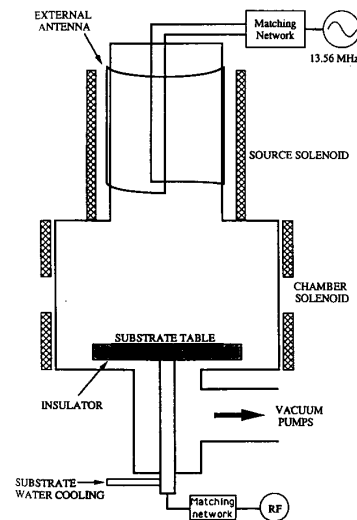


Fig. 72. Schematic of a helicon wave source [47].

### E. The Tokamak H-Mode

The discovery of the H-mode drew attention to the importance of transverse electric fields, and the difference in behavior of L-mode and H-mode discharges should give clues as to how the fields at the edge layer can affect plasma stability. Unfortunately, tokamaks do not provide a clean environment for basic experiments, since the magnetic field lines are not straight, and the plasma may have many charged and neutral species in the limiter region. In a uniform magnetic field, at least three mechanisms are involved with plasma stability in a transverse  $\mathbf{E}$ -field: differential  $\mathbf{E} \times \mathbf{B}$  drifts, Kelvin-Helmholtz effects due to electric shear, and drift wave effects due to pressure gradients. Note that the  $\mathbf{E} \times \mathbf{B}$  effect can be strongly stabilizing in those regions where the sign is opposite to that in the reflex arc. These effects can be separated by proper experimental design, provided that the complicating factors of magnetic shear, trapped particles, etc. are eliminated. Consider the simple apparatus shown in Fig. 67. As discussed later, a helicon source can create highly ionized, quiescent plasmas in the  $10^{13}$ – $10^{14} \text{ cm}^{-3}$  density range with just a few kilowatts of rf power. When put into a PISCES-type machine with a biasable aperture limiter, such a plasma can simulate the edge layer of the H-mode. In inertial fusion, we were able to isolate and understand the various parametric instabilities by doing specially designed experiments using specially tailored plasma sources. If basic experiments in magnetic fusion were still supported, the physics of the H-mode edge layer could be understood much better than it is now.

## IV. TECHNOLOGICAL PLASMAS FOR THE FUTURE

### A. Applications of Plasma Processing

Even as funding for the traditional areas of plasma physics declines, the use of plasmas in manufacturing is rapidly



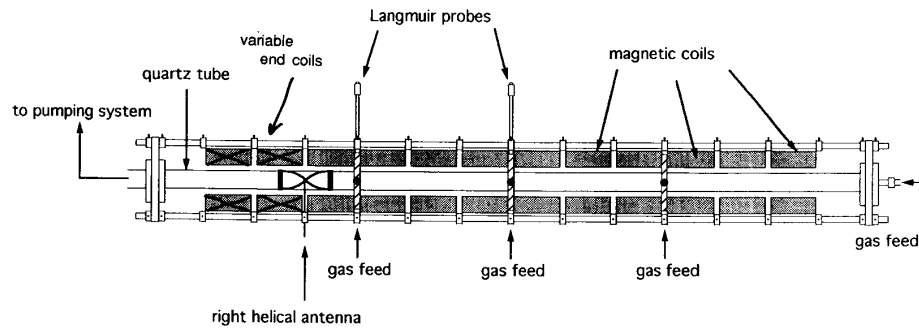


Fig. 73. Device for basic studies of helicon discharges.

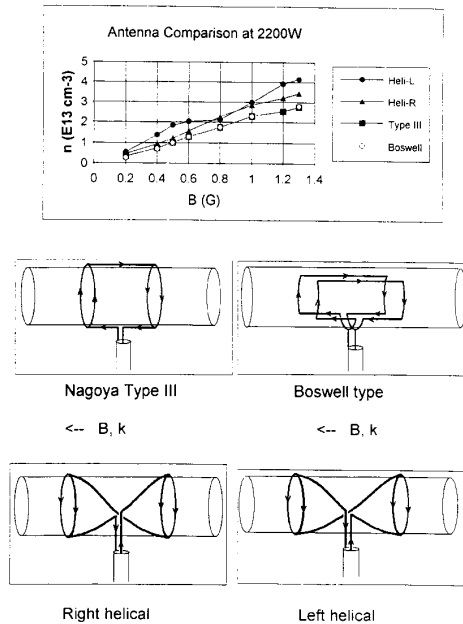


Fig. 74. Peak densities obtained with different helicon antennas versus magnetic field [48].

expanding. There is a resurgence of low-temperature plasma physics, a field formerly called Gaseous Electronics. Only a short list of industrial plasma applications can be given here:

#### Semiconductor fabrication

Etching, deposition, cleaning  
 Problems: uniformity, dust, oxide damage

#### Deposition and polymerization

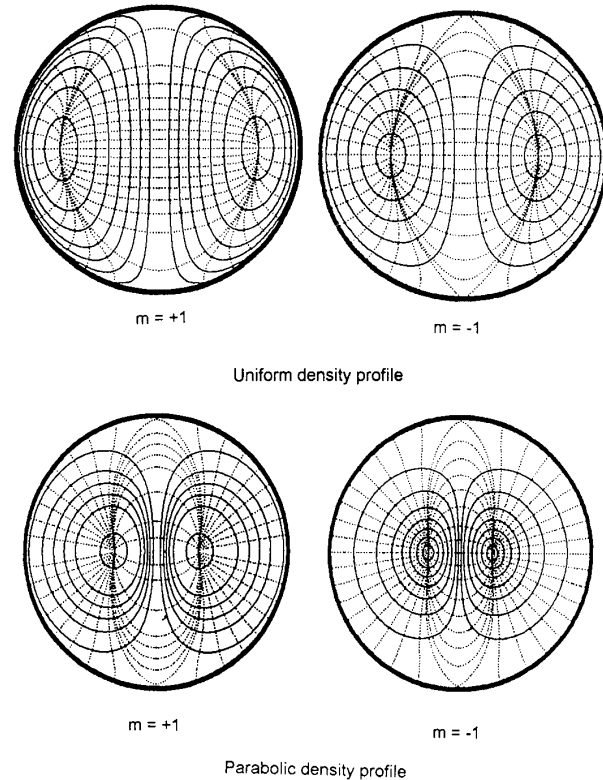
Optical fibers, coatings  
 Barrier coatings  
 Treatment of fibrous materials

#### Surface modification

Ion implantation  
 Corrosion resistance  
 Diamond films  
 Magnetic and optical disks

#### Flat panel displays

AMLCD's, plasma displays, EL, FED  
 Computers, cockpits, dashboards, TV

Fig. 75. Computed helicon mode patterns for right- and left-hand polarized modes ( $m = +1, -1$ ) for uniform and parabolic density profiles [49].

#### High pressure arcs and jets

Ceramic coatings  
 Wire arc spraying  
 Diamond films

#### B. Plasma Sources for Industrial Applications

Though most of the problems in plasma processing concern chemical and surface physics phenomena, nothing can be done unless a plasma is properly produced in the first place. The development of new plasma sources is only now becoming an active area of research. By far the most common plasma source is the radiofrequency parallel-plate capacitive discharge, called the RIE (Reactive Ion Etching) discharge shown schematically

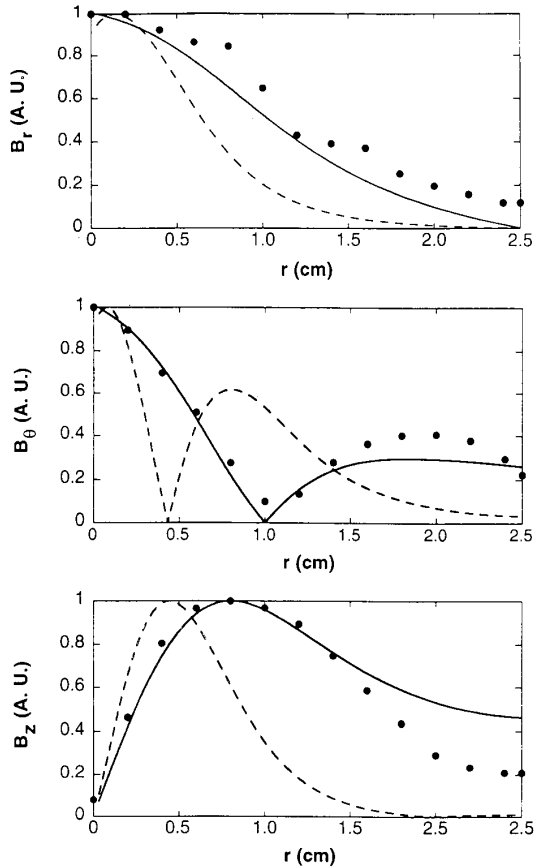


Fig. 76. Measured components of the wave magnetic field (points) compared with theoretical profiles for the  $m = +1$  (solid line) and  $m = -1$  (dashed line) modes in a helicon discharge [49].

in Fig. 68 [41]. Semiconductor manufacturers have billions of dollars invested in "reactors" using this source, and the source has been studied extensively in experiment and computer modeling. Its greatest virtue is simplicity. However, it may not be the best way to generate a plasma for all purposes, and a number of alternate concepts have been proposed. Foremost among these is the ECR source (Fig. 69) [42], an outgrowth of ECRF heating in magnetic fusion research. Its greatest drawback is the 875 G field needed at 2.45 GHz. Both of these sources can be coupled to a MacKenzie bucket. A newer invention is the RFI (RadioFrequency Inductive) discharge, also called the TCP (Transformer Coupled Plasma), shown in Fig. 70 [43]. It can cover a large area uniformly without using a magnetic field. There are also various inductively coupled plasmas in which the rf is applied via an electrostatically shielded helix (Fig. 71) [44]. Understanding and optimizing such plasma sources can be an interesting new direction for basic plasma research.

### C. Development of the Helicon Source

At UCLA, we have been concentrating on the helicon source, which I got interested in because it has a higher

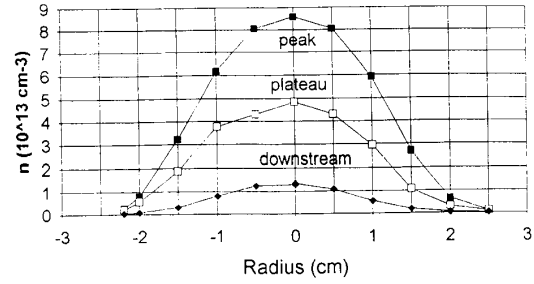


Fig. 77. Peak density in units of  $10^{13} \text{ cm}^{-3}$  in a helicon discharge. Gas depletion causes the lower curve marked "plateau."

ionization efficiency than any other source and has more flexibility. Helicon waves in plasmas are low-frequency whistler waves confined to a cylinder; they were first found by Peter Thonemann and his colleagues [45] in England. Later, Boswell [46] discovered in Australia that helicon discharges produced very dense plasmas. It was in Australia that I discovered Boswell and suggested that the ionization process might involve Landau damping [47]. Fig. 72 shows a diagram of a helicon source [48] applied to semiconductor etching or deposition, and Fig. 73 shows the apparatus we have used [49] the past few years to study the physics of helicon discharges. Some of the possible advantages of helicon sources are as follows:

- High density, high efficiency
- Uniformity and quiescence
- Low neutral pressure
- Low  $B$ -field relative to ECR
- No internal electrodes
- Control of electron and ion energies
- Remote operation, good access
- Self-generated dc wafer bias

It has been fascinating and exciting research; we have verified theory in some cases and found unexpected effects in others. A few examples will suffice. Fig. 74 shows several antennas we have used and the peak densities obtained with them. The helical ones give higher densities and are supposed to excite  $m = +1$  and  $-1$  modes. We have computed the mode patterns for these modes in uniform and nonuniform density plasmas; the results are shown in Fig. 75. The  $m = -1$  mode seems to concentrate the RF energy into a smaller volume near the axis, explaining why the left-hand helical (L) antenna gives the highest density. When we actually measured the mode patterns with a magnetic probe, however, we found that all antennas excited the  $m = +1$  mode (Fig. 76) [50]. This discrepancy is still under study. When we reverse the end coils of the solenoid and place the antenna in a magnetic cusp field, we found a beneficial five-fold increase in axial density. After a long series of experiments, we believe that this is due to the magnetic aperture limiter effect, coupled with the destruction of the backward-going helicon wave. Fig. 77 shows the density profile at high pressure with the cusp field; note that the peak is nearly  $10^{14} \text{ cm}^{-3}$  even though there is not axial confinement. Recent measurements [51] of the axial variations of density, electron temperature, space potential,

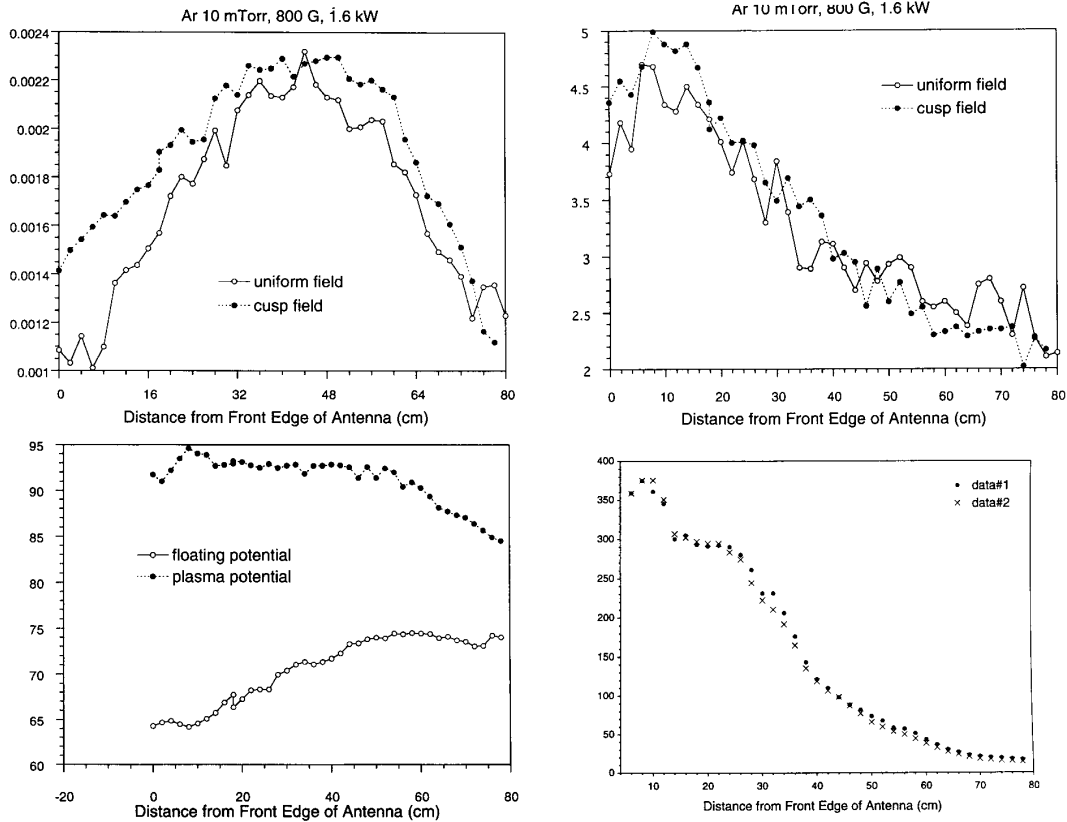


Fig. 78. Axial variations of density, electron temperature, space and floating potential, and ionized Argon light in a helicon discharge (I. Sudit and F. F. Chen, to be published.).

and 488-nm Ar<sup>+</sup> light are shown in Fig. 78. It was at first surprising that the density should increase with distance away from the antenna. However, the other curves show that  $KT_e$  drops, as it should, and therefore the density has to increase to maintain pressure balance. The floating potential also rose unexpectedly, but when it is corrected to the space potential, we see that the latter is flat, agreeing with the  $E_{\parallel} = 0$  condition. The optical emission curve shows a falloff that is too slow to agree with the temperature profile, but if one assumes that metastables are created near the antenna and drift downstream, then the cold electrons there can ionize them and produce the observed curve. Studies of this kind show that basic plasma physics is still alive, and that industrial plasmas do not have to be treated in a rough and ad hoc fashion.

## V. CONCLUSION

As plasma physics moves into the 21st century, I have no doubt that its main impact on society will come through its industrial applications, at least until fusion power becomes prevalent in the latter half of that century. Following the historical trend, as we have shown in this talk, the development of technological plasmas will no doubt be spearheaded by the invention of new plasma sources.

## REFERENCES

- [1] F. Boeschoten and F. Schwirzke, *Nuclear Fusion*, vol. 2, p. 54, 1962.
- [2] J. Malmberg and C. Wharton, *Phys. Rev. Lett.*, vol. 17, p. 175, 1966.
- [3] J. M. Wilcox, W. R. Baker, F. I. Boley, W. S. Cooper III, A. W. deSilva, and G. R. Spillman, *J. Nucl. Energy*, pt. C, vol. 5, p. 337, 1962.
- [4] J. M. Wilcox, F. I. Boley, and A. W. deSilva, *Phys. Fluids*, vol. 3, p. 15, 1960.
- [5] R. Taylor, K. MacKenzie, and H. Ikezi, *Rev. Sci. Instrum.*, vol. 43, p. 1675, 1972.
- [6] R. Taylor, D. Baker, and H. Ikezi, *Phys. Rev. Lett.*, vol. 24, p. 206, 1970.
- [7] H. Ikezi, R. J. Taylor, and D. R. Baker, *Phys. Rev. Lett.*, vol. 25, p. 11, 1970.
- [8] B. H. Quon and A. Y. Wong, *Phys. Rev. Lett.*, vol. 37, p. 1393, 1976.
- [9] B. H. Ripin and R. L. Stenzel, *Phys. Rev. Lett.*, vol. 30, p. 45, 1973.
- [10] R. Limpacher and K. R. MacKenzie, *Rev. Sci. Instrum.*, vol. 44, p. 726, 1973.
- [11] R. L. Stenzel, *Phys. Rev. Lett.*, vol. 9, p. 547, 1975; *Phys. Fluids*, vol. 19, p. 857, 1976.
- [12] R. L. Stenzel, A. Y. Wong, D. Arnush, B. D. Fried, and C. F. Kennel, AGARD-NATO Meeting CTP-138, no. 4-1, 1973.
- [13] R. L. Stenzel, W. Gekelman, and M. Urrutia, *Adv. in Space Res.*, vol. 6, p. 135, 1986.
- [14] R. L. Stenzel, W. Gekelman, and N. Wild, *Phys. Fluids*, vol. 26, p. 1949, 1983.
- [15] C. L. Rousculp, R. L. Stenzel, and J. M. Urrutia, *Phys. Rev. Lett.*, vol. 72, p. 1658, 1994; J. M. Urrutia, R. L. Stenzel, and C. L. Rousculp, *Geophys. Res. Lett.*, vol. 21, p. 413, 1994.
- [16] W. Gekelman, J. E. Maggs, and H. Pfister, *IEEE Trans. Plasma Sci.*, vol. 20, p. 614, 1992.
- [17] N. Rynn and N. D'Angelo, *Rev. Sci. Instrum.*, vol. 31, p. 1326, 1960.
- [18] H. Hendel, T. K. Chu, and P. Politzer, *Phys. Fluids*, vol. 11, p. 2426, 1968.

- [19] R. W. Motley and N. D'Angelo, *Phys. Fluids*, vol. 6, p. 296, 1963.
- [20] A. Y. Wong, R. W. Motley, and N. D'Angelo, *Phys. Rev. A*, vol. 133, p. 436, 1964.
- [21] P. J. Barrett, H. G. Jones, and R. N. Franklin, *Plasma Phys.*, vol. 10, p. 911, 1968.
- [22] J. J. Turechek and F. F. Chen, *Phys. Rev. Lett.*, vol. 36, p. 720, 1976.
- [23] M. J. Herbst, C. E. Clayton, and F. F. Chen, *Phys. Rev. Lett.*, vol. 43, p. 1591, 1979; *J. Appl. Phys.*, vol. 51, p. 4080, 1980.
- [24] B. Amini and F. F. Chen, *Phys. Fluids*, vol. 29, p. 3864, 1986.
- [25] ———, *Phys. Rev. Lett.*, vol. 53, p. 1441, 1984.
- [26] C. Joshi, C. E. Clayton, and F. F. Chen, *Phys. Rev. Lett.*, vol. 48, p. 874, 1982.
- [27] F. C. Hoh and B. Lehnert, *Phys. Fluids*, vol. 3, p. 600, 1960.
- [28] F. Chen, J. File, and E. W. Lehmann, *Project Matterhorn*, Tech. Memo 68, NYO-8071, 1959.
- [29] F. F. Chen, *Rev. Sci. Instrum.*, vol. 40, p. 1049, 1969.
- [30] A. Simon, *Phys. Fluids*, vol. 6, p. 382, 1963.
- [31] R. Bingham, F. F. Chen, and W. Harries, PPL MATT-63, 1962; F. F. Chen, PPL MATT-249, 1964.
- [32] F. F. Chen, *Phys. Rev. Lett.*, vol. 8, p. 234, 1962.
- [33] R. D. Lehmer, private communication.
- [34] D. Mosher and F. F. Chen, *Phys. Fluids*, vol. 13, p. 1238, 1970.
- [35a] F. F. Chen and K. C. Rogers, Princeton Plasma Lab. Rep., MATT-701, 1969.
- [35b] F. F. Chen, in *Proc. Int. Conf. on Phys. of Quiescent Plasmas*, Paris, France, vol. II, p. 159, 1969.
- [36] F. F. Chen, D. Mosher, and K. C. Rogers, in *Proc. 1968 IAEA Int. Conf. on Plasma Phys. and Controlled Nuclear Fusion Research*, vol. 1, p. 625, 1969.
- [37] Y. Sakawa, C. Joshi, P. K. Kaw, F. F. Chen, and V. K. Jain, *Phys. Fluids*, vol. B-5, p. 1681, 1993.
- [38] Y. Sakawa, C. Joshi, P. K. Kaw, V. K. Jain, T. W. Johnston, F. F. Chen, and J. M. Dawson, *Phys. Rev. Lett.*, vol. 69, p. 85, 1992.
- [39] F. F. Chen, in *Proc. Int'l Conf. on Plasma Physics*, Innsbruck, vol. III, p. 1789, 1992.
- [40] F. F. Chen and M. J. Hsieh, in *Proc. Int. Workshop on Magnetic Turbulence and Transport*, Cargèse, France, p. 56, 1992.
- [41] D. M. Manos and D. L. Flamm, *Plasma Etching*, New York: Academic, 1989.
- [42] N. Sadeghi, T. Nakano, D. J. Trevor, and R. A. Gottscho, *J. Appl. Phys.*, vol. 70, p. 2552, 1991.
- [43] J. Hopwood, *Plasma Sources Sci. Technol.*, vol. 1, p. 109, 1992.
- [44] W. L. Johnson, in *Proc. 36th Techn. Conf. Soc. Vacuum Coaters*, 1993.
- [45] J. A. Lehane and P. C. Thonemann, *Proc. Phys. Soc.*, vol. 85, p. 301, 1965.
- [46] R. W. Boswell, *Phys. Lett.*, vol. 33, p. 457, 1970.
- [47] F. F. Chen, *Plasma Phys. and Controlled Fusion*, vol. 33, p. 339, 1991.
- [48] A. J. Perry, D. Vender, and R. W. Boswell, *J. Vac. Sci. Technol. B*, vol. 9, p. 310, 1991.
- [49] F. F. Chen and G. Chevalier, *J. Vac. Sci. Technol. A*, vol. 10, p. 1389, 1992.
- [50] M. Light, M.S. thesis, UCLA, 1994.
- [51] I. D. Sudit and F. F. Chen, *Bull. Amer. Phys. Soc.*, vol. 39, p. 1727, 1994.



**Frank Chen** (SM'72–F'80) began his 40-year career as a plasma physicist when he was hired by Lyman Spitzer, Jr., in 1954 as one of the first 15 employees at Project Matterhorn, now known as the Princeton Plasma Physics Laboratory. He worked there for 15 years on plasma diagnostics, magnetic fusion, and basic plasma physics. Since 1969 he has been Professor of Electrical Engineering, University of California at Los Angeles, Los Angeles, where he established the plasma curriculum in engineering, as well as research programs in far-infrared laser diagnostics, CO<sub>2</sub> laser-plasma interactions, and, most recently, plasma processing.